



저작자표시-비영리-변경금지 2.0 대한민국

이용자는 아래의 조건을 따르는 경우에 한하여 자유롭게

- 이 저작물을 복제, 배포, 전송, 전시, 공연 및 방송할 수 있습니다.

다음과 같은 조건을 따라야 합니다:



저작자표시. 귀하는 원저작자를 표시하여야 합니다.



비영리. 귀하는 이 저작물을 영리 목적으로 이용할 수 없습니다.



변경금지. 귀하는 이 저작물을 개작, 변형 또는 가공할 수 없습니다.

- 귀하는, 이 저작물의 재이용이나 배포의 경우, 이 저작물에 적용된 이용허락조건을 명확하게 나타내어야 합니다.
- 저작권자로부터 별도의 허가를 받으면 이러한 조건들은 적용되지 않습니다.

저작권법에 따른 이용자의 권리는 위의 내용에 의하여 영향을 받지 않습니다.

이것은 [이용허락규약\(Legal Code\)](#)을 이해하기 쉽게 요약한 것입니다.

[Disclaimer](#)

공학박사 학위논문

Toward Reliable Broadcast/Unicast in Wireless Mobile Ad Hoc Networks

무선 이동 애드 혹 네트워크에서 안정적인
브로드캐스트/유니캐스트 서비스를 위한 라우팅
프로토콜 설계

2016 년 2 월

서울대학교 대학원

전기·컴퓨터공학부

강 대 호

Toward Reliable Unicast/Broadcast in Wireless
Mobile Ad-hoc Networks

Daeho Kang

Ph.D. Dissertation

Abstract

A mobile ad-hoc network (MANET) is a dynamic, self-organizing network that is composed of numerous mobile devices scattered in a particular area. Each device is equipped with a wireless transceiver for physical-layer communication. In MANET, data traffic should traverse intermediate nodes between the source and the destination due to the limited communication range of devices. In this dissertation, we develop routing schemes for reliable and scalable broadcast/unicast communication service in MANETs.

First, we develop efficient broadcast protocol, named ST-BCAST, that exploits collision resilient tone-signals and employs receiver triggered forwarding decision / cancellation mechanism. It reliably disseminates a packet over MANET without any topological information. We verify the reliability and efficiency of ST-BCAST through logical analysis and NS-3 based simulations.

Second, we investigate two well-known classes of routing mechanisms for unicast service in MANET: hop-by-hop routing and gradient routing. We evaluate their performance under realistic MANET en-

vironments with unreliable links and node mobility. Based on the understanding of their behaviors, we propose a practical gradient forwarding architecture (E-GRAD) that includes on-demand cost update and SNR-based cost calculation. We demonstrate that the performance of E-GRAD is closed to that of the ideal routing scheme with global information.

Last, we consider wireless multi-hop access networks with a single gateway, e.g., sensor networks and smart-phone based disaster recovery networks, and design novel gradient routing schemes for uplink/downlink unicast services. In our proposed scheme, every node can efficiently calculate the routing cost to the gateway by relaying a tone signal across subcarriers, where a cost value (e.g., hop count to the gateway) is pre-assigned to each subcarrier. The cost calculation is initiated by the gateway and is computed as the signal propagates to the network boundary. For uplink gradient routing, the cost can be used directly, and for downlink gradient routing, the cost is used in conjunction with uplink transmission history. We verify through NS-3 simulations that our proposed single-gateway routing scheme provides reliable uplink and downlink traffic, and substantially reduces the routing overhead by successfully exploiting OFDM signals.

Keywords: MANET, routing, unicast, broadcast, tone-signal

Student Number: 2010-20743

Contents

1	Introduction	1
1.1	Background	1
1.2	Contributions and outline	3
2	ST-BCAST: An Efficient Broadcast Protocol using Subcarrier-	
	level Tone-signals	6
2.1	Introduction	6
2.2	System model	10
2.3	ST-BCAST	12
2.3.1	Control signals	12
2.3.2	Forwarding state lists	13
2.3.3	Receiver-triggered forwarding decision and can-	
	cellation	15
2.3.4	Operation example	17
2.3.5	Mode switching mechanism for multiple source	
	case	19

2.3.6	Physical layer aspects for RTF and FR transmission and detection	20
2.3.7	Duration of RTF and FR	21
2.4	Reliability of ST-BCAST	21
2.5	Feasibility of tone signal detection	25
2.6	Simulation results	28
2.6.1	Implementation	28
2.6.2	Broadcast schemes in comparison	29
2.6.3	Performance metrics	30
2.6.4	Simulation environments	31
2.6.5	Results - single source	33
2.6.6	Results - multiple sources	38
2.7	Related Work	40
2.8	Summary	43
3	E-GRAD: Revisiting Gradient Routing Protocol for Reliable Unicast in MANET	44
3.1	Introduction	44
3.2	Forwarding mechanisms for unicast transmission	47
3.2.1	Hop-by-hop routing	47
3.2.2	Gradient routing	49
3.3	Reliability analysis of hop-by-hop routing and gradient routing	51
3.3.1	Impact of errors in link quality estimation	52

3.3.2	Impact of node mobility	54
3.4	E-GRAD: A practical greedy routing architecture for MANET	57
3.4.1	On-demand flooding-based cost update protocol	57
3.4.2	SNR-based cost allocation	61
3.4.3	Miscellaneous for efficient forwarding cancellation	64
3.5	Simulation results	65
3.5.1	System model	65
3.5.2	Schemes in comparison	68
3.5.3	Performance metrics	70
3.5.4	Simulation environments	70
3.5.5	Results	71
3.6	Related work	84
3.7	Summary	85
4	Access-GRAD: A Gradient Routing Protocol for Up- link and Downlink Unicast in Wireless Multi-hop Ac- cess Networks	86
4.1	Introduction	87
4.2	System model	89
4.3	Access-GRAD	90
4.3.1	Tone-signal based cost update	90
4.3.2	History based gradient routing for downlink trans- mission	93

4.4	Performance evaluation	95
4.4.1	Uplink performance	98
4.4.2	Downlink performance	101
4.5	Summary	103
5	Conclusion	104
5.1	Research contributions	104
5.2	Future research directions	106

List of Tables

2.1	Simulation parameters used for ST-BCAST	29
4.1	System parameters of the proposed scheme	97

List of Figures

2.1	An example of protocol operation when node S wants to flood a broadcast packet $P(i)$. In this example, the number of available subcarriers is 4.	17
2.2	The testbed consisting of three USRP hosts. The right most host acts as a tone-signal detector (RX1). The other two hosts (TX1, TX2) act as tone-signal transmitters.	25
2.3	The squared magnitude of frequency-domain samples calculated at RX1 when TX1 transmits a tone-signal on subcarrier 40. We can see that there is a peak near 40th subcarrier.	26
2.4	The change of the squared magnitude of frequency-domain samples on the subcarrier 40. For each point, 256 time-domain samples are fed into FFT calculator.	27
2.5	Single source - Packet delivery ratio with different node density	33

2.6	Single source - Communication overhead with different node density	34
2.7	Single source - Average number of additional FR transmissions with different node density	35
2.8	Single source - Average packet delivery time with different node density	36
2.9	Single source - Packet delivery ratio with different signal detection error probabilities	37
2.10	Single source - Communication overhead with different signal detection error probabilities	38
2.11	Multiple sources - Packet delivery ratio with different number of broadcast sources	39
2.12	Multiple sources - Communication overhead with different number of broadcast sources	40
3.1	An example scenario where node <i>A</i> is trying to forward a packet destined to node <i>D</i> through gradient forwarding.	52
3.2	The operation of hop-by-hop routing and gradient routing when there is an active session between node <i>S</i> and node <i>D</i> . Node <i>A</i> moves out from the route while the session is active.	56
3.3	Signaling messages used in E-GRAD.	57
3.4	The operation flow diagram of node when it receives an URM.	58

3.5	The operation flow diagram of node when it receives an UM.	59
3.6	The operation flow diagram of node when it receives an UBTM.	60
3.7	An example of MANET scenario. Node A is a traffic source, and node D is a traffic destination. In this example, the link between node A and node C is unreliable.	63
3.8	Packet delivery ratio under different fading coefficients.	72
3.9	The average number of forwarder candidates for a node with forwarding schedule. In E-GRAD, more number of nodes participate in packet forwarding compared to GRAD (Hop).	72
3.10	The accumulated number of delivered packets for a randomly-chosen end-to-end session as the simulation time elapses. We can see that E-GRAD delivers most of generated packets without bursty losses.	73
3.11	The ratio of invalid operation events to all corresponding events. The ratio of invalid forwarding cancellations and denials is smaller in E-GRAD than in GRAD (Hop).	74
3.12	The number of transmissions used for data traffic delivery under different fading coefficients.	76
3.13	The average end-to-end delay of routing protocols under different fading coefficients.	77

3.14	The packet deliver of routing protocols under different node mobility.	78
3.15	The accumulated number of delivered packets for a randomly-chosen end-to-end session as the simulation time elapses. Here, the speed of nodes are chosen within [1,9] m/s. We can confirm that E-GRAD provides reliable unicast service even though there are errors in the estimated cost.	79
3.16	The number of transmissions used for data traffic delivery under different node mobility.	80
3.17	The average end-to-end delay of routing protocols under different node mobility.	81
3.18	The number of received packets according to the traveled hop count.	81
3.19	The average number of network-layer retransmissions in the procedure of gradient routing. GRAD (Hop) yields more number of retransmissions than E-GRAD.	82
3.20	The average per-session throughput with different offered load.	83
3.21	The average end-to-end delay with different offered load.	83
4.1	A smart-phone based disaster recovery network. A live base station and mobile devices can communicate with each other multi-hop wireless links.	89

4.2	The operation flow diagram of node A when it detects a tone-signal on subcarrier i	92
4.3	The structure of the simulator. We implemented a gradient routing module in the network layer, and a tone-signal manager block in the MAC layer.	97
4.4	The average packet delivery ratio of uplink sessions with different node mobility.	99
4.5	The average number of transmissions for uplink sessions with different node mobility.	100
4.6	The average end-to-end delay of uplink traffic with different node mobility.	100
4.7	The average packet delivery ratio of downlink sessions with different node mobility.	101
4.8	The average number of transmissions for downlink sessions with different node mobility.	102
4.9	The average end-to-end delay of downlink traffic with different node mobility.	102

Chapter 1

Introduction

1.1 Background

A mobile ad-hoc network (MANET) is a dynamic, self-organizing network that consists of numerous mobile devices with wireless communication capability. There are many promising services that demand practical deployment of MANETs: military tactical networking [1], vehicular networking [2], smart-phone based disaster recovery networks [27], and large-scale mobile sensor networks [3]. In MANETs, every node operates as a network router since they cannot communicate directly with each other due to limited wireless transmission range.

Most applications rely on either unicast or broadcast transmissions. Unicast is a communication service primitive that sends a message from a single source to a specific destination identified by a unique

address. Many Internet applications, e.g., file transfer, media streaming, text messaging, and web browsing, use unicast to deliver their contents to the destination. Broadcast is another type of communication service primitive that aims for disseminating information from the source to all the other nodes in the network. In MANETs, the broadcast service is widely used to find unknown destination nodes in routing protocols [4, 6], disseminating emergency messages [10], and performing network-wide firmware updates [11].

On providing reliable unicast service in MANET, there are two major challenges: node mobility and estimation errors of link quality. The node mobility incurs frequent changes of network topology and thus decreases the lifetime of routing paths. On the other hand, the estimation error of link quality, often caused by multi-path propagation, Doppler effect, and interferences[22], leads to wrong routing decision. The routing protocol should handle these two challenges accordingly in order to provide unicast service in a reliable and efficient manner.

For the broadcast service, it is imperative to achieve high packet delivery ratio and to minimize the usage of communication resources. Flooding is the most widely used mechanism for the broadcast service. In the flooding, the node that receives a new broadcast packet simply forwards it, with some waiting time to avoid collisions [29]. While it is simple and robust to the estimation errors, it suffers from high overhead due to unnecessary retransmissions especially in dense networks,

where high degree of collisions causes waste of resources [41]. Further, it cannot guarantee the packet delivery due to lack of feedback mechanism, e.g., link-level acknowledgment. A number of protocols have been proposed to improve reliability and efficiency of broadcast in MANET. They include probabilistic forwarding decision [44], per-neighbor feedback [36], topology information piggyback [37], the concurrent transmissions of the same packet [20], or a combination of these options. However, their performance gain is incremental and limited to provide a tradeoff between the reliability and the efficiency, rather than achieving substantial improvement in both dimensions.

1.2 Contributions and outline

In this dissertation, we develop reliable and scalable routing schemes for broadcast/unicast communication service in MANETs by carefully addressing the challenges of node mobility and link-quality estimation errors. For broadcast service, we develop Subcarrier-level Tone-signal based Broadcast (ST-BCAST) that successfully combines collision-resilient tone-signals with receiver-triggered forwarding decision / cancellation mechanism. For reliable unicast service, we develop an Enhanced version of gradient routing (E-GRAD) that blends the scheme with on-demand cost updates and SNR-based cost calculation. Finally, we propose a gradient routing protocol for wireless multi-hop access networks (Access-GRAD) that supports efficient uplink and

downlink unicast services.

This dissertation is organized as follows.

In Chapter 2, we propose a scalable broadcast protocol, named Subcarrier-level Tone-signal based broadcast (ST-BCAST), that disseminates a packet over OFDM-based wireless multi-hop networks in an efficient and reliable manner. Exploiting collision-resilient tone-signals and receiver-triggered forwarding decision/cancellation, ST-BCAST achieves both high packet delivery ratio and low communication overhead without using any topological information, thereby providing a scalable solution to the network size. Under a mild assumption, ST-BCAST satisfies two sufficient conditions for reliable broadcasting: first-hop delivery condition and successful relay condition. We verify the feasibility of tone-signal generation and detection through experiments using Universal Software Radio Peripheral (USRP) devices, and show through NS-3 simulations that ST-BCAST significantly outperforms the state-of-the-art broadcast schemes in terms of packet delivery ratio and communication overhead.

In Chapter 3, we propose an enhanced gradient routing (E-GRAD) that exploits on-demand cost update procedure with SNR-based cost calculation. We start with investigating the performance of two well-known routing schemes, hop-by-hop routing and gradient routing, under realistic MANET environments. We observe potential advantages of gradient routing, and design E-GRAD that successfully inherits the advantages of gradient routing by carefully combining it with on-

demand cost update and SNR-based cost calculation. Finally, we demonstrate that E-GRAD greatly outperforms the state-of-the-art schemes and its performance is even comparable with the ideal routing scheme using global topology information.

In Chapter 4, we consider a multi-hop wireless access networks with a single gateway which can model a wide class of applications, including smart-phone based disaster recovery networks. We extend our E-GRAD to support efficient and reliable uplink and downlink access to the gateway. In our proposed scheme, every node can efficiently calculate the routing cost to the gateway by relaying a tone signal across subcarriers, where a cost value (e.g., hop count to the gateway) is pre-assigned to each subcarrier. The cost calculation is initiated by the gateway and is computed as the signal propagates to the network edge. For uplink routing, the cost can be used directly, and for downlink routing, the cost is used in conjunction with uplink transmission history. We verify through NS-3 simulations that our proposed single-gateway routing scheme provides reliable uplink and downlink traffic, and substantially reduces the routing overhead by successfully exploiting OFDM signals.

We conclude the dissertation in Chapter 5.

Chapter 2

ST-BCAST: An Efficient Broadcast Protocol using Subcarrier-level Tone-signals

2.1 Introduction

Network-wide packet broadcast is a communication service that aims to disseminate a packet from a source node to all the other nodes in the network. It has been widely used in wireless multi-hop networks for various purposes. For example, on-demand routing protocols such as AODV [4] utilize broadcast service to find a route from a source

node to a destination node. The broadcast service is also used in vehicular ad-hoc networks for emergency message dissemination [10], and in wireless sensor networks for code update [11] and network-wide information dissemination [26].

A typical way of packet broadcast in wireless multi-hop networks is flooding: a node that receives a broadcast packet forwards it after some random backoff time [29]. The advantage of this method is its simplicity and robustness of the operation. However, it can cause numerous unnecessary retransmissions especially in dense networks, resulting in high degree of collisions and waste of resources [41], and does not guarantee the packet delivery. Hence, the reliability and efficiency of the simple flooding scheme highly depend on network topology.

A number of protocols have been proposed for reliable and efficient network-wide packet broadcast. For reliable broadcast, many protocols exploit feedback messages from medium access control (MAC) or network layers to guarantee the delivery of the broadcast packet to neighboring nodes [30, 31, 33, 32, 34, 35, 36, 37]. However, they are not scalable with respect to node density since communication overhead for feedback message exchange increases with the degree of node connectivity. In addition, reacting to per-neighbor feedback can incur severe retransmission overhead since a node can have a number of neighbors with weak link condition. In this case, finding a different packet forwarder may be more appropriate.

Regarding the efficiency, previous work can be grouped into two categories: counter-based schemes and probability-based schemes [45, 41, 62]. Under counter-based schemes, when a node receives a broadcast packet, it schedules its transmission after a random backoff time, and in the meantime, overhears neighbors' transmission and counts the number of transmissions for it. If the number of overheard transmissions is beyond a threshold, the node cancels its transmission, which helps to remove unnecessary transmissions of the packet. However, the broadcast may terminate incompletely since overhearing multiple packet transmissions does not imply that all its neighboring nodes have received the packet successfully. Under probability-based schemes, when a node receives a broadcast packet, it makes a forwarding decision with probability p . The value of p can be either the same for all nodes [44, 41] or different according to topological information, such as the number of neighbors [40]. Unfortunately, the probability-based schemes do not guarantee complete delivery of the packet since a forwarder who is essential for reliable broadcast rejects to forward the received packet with probability $1 - p$.

In this chapter, we propose a scalable broadcast protocol that achieves both high reliability and efficiency without using any topological information in orthogonal frequency division multiplexing (OFDM) based wireless multi-hop networks. Smartphone based ad-hoc disaster recovery network [27, 28], where emergency messages are frequently broadcasted, can be a good example application. The main idea is to

make a node forward a received broadcast packet only if it detects an explicit forwarding request from its neighbors.

To this end, we introduce a receiver-triggered forwarding decision and a forwarding cancellation mechanism, which are intended to provide reliability and efficiency, respectively. Our scheme uses two control signals, named ready-to-forward (RTF) and forward-request (FR). RTF is used to advertise the presence of a broadcast packet, while FR is used to request the forwarding of it. We further reduce the communication overhead for RTF/FR transaction by allowing overlapped transmissions of RTF and FR. RTF and FR are subcarrier-level tone-signals that can be detected by receivers through energy detection, even when multiple nodes transmit either RTF or FR simultaneously.

In order to verify how our subcarrier-level tone-signal based broadcast protocol (ST-BCAST) provides reliable packet delivery, we show that ST-BCAST satisfies two sufficient conditions, i.e., first-hop delivery condition and successful relay condition, for the completion of a packet broadcast under a mild assumption. Then, we confirm the feasibility of tone-signal generation and detection capability through experiments using USRP devices [63]. Finally, we show that ST-BCAST outperforms conventional broadcast schemes in terms of packet delivery ratio and communication overhead through extensive simulations using NS-3. While the other comparable broadcast schemes have communication overhead that increases linearly with node density, ST-

BCAST maintains a constant overhead beyond a certain level of node density.

The rest of the paper is organized as follows. In Section 2.2, we briefly describe the system model. In Section 2.3, we explain ST-BCAST in detail. In Section 2.4, we analyze the reliability of ST-BCAST logically. Section 2.5 evaluates the feasibility of subcarrier-level tone-signal transmission and detection through experiments using USRP devices. In Section 2.6, we provide simulation results in comparison with other broadcast schemes. Section 2.7 discusses related work. Finally, we summarize this chapter in Section 2.8.

2.2 System model

We consider a wireless multi-hop network with a set V of wireless nodes. Each node has a half-duplex OFDM transceiver [61, 59]. The channel bandwidth is W , and the size of the Fast Fourier Transform (FFT) window (i.e., the number of subcarriers) is N_{FFT} . Among N_{FFT} subcarriers, we use N_S ($< N_{FFT}$) subcarriers for transmission of data symbols or tone-signals. We assume that all nodes transmit with the same power and data rate.

Each node detects transmission of a packet or a tone-signal by measuring the energy on the channel spectrum. Specifically, we assume that subcarrier-level energy detection is possible: if node $v \in V$ transmits a tone-signal on a subcarrier j , then the nodes located

within the transmission range of node v detect the signal transmission and identify subcarrier j . This subcarrier-level tone-signal transmission and detection capability has been shown to be feasible in the literature [34, 42, 43].

For an interference model, we use the graded signal-to-interference-plus-noise ratio (SINR) model that reflects a practical wireless link with non-binary reception success probability (RSP)[57]. Under this interference model, the RSP of a link is determined by the SINR value at the receiving node. Suppose that node $v \in V$ transmits a frame to node $w \in V$. Then, the SINR at node w is

$$SINR_w = \frac{P_{vw}}{N + \sum_{k \in V \setminus v} P_{kw}}, \quad (2.1)$$

where P_{vw} is the received power of node v 's transmission at node w , N is the thermal noise floor, and P_{kw} is the interference experienced at node w due to the transmission of node k . If the SINR is greater than a threshold β , then the RSP is almost 1. RSP at a link gradually decreases down to zero as the SINR becomes lower.

For wireless channel access, every node operates carrier sense multiple access / collision avoidance (CSMA/CA) mechanism [60]. Under CSMA/CA, a node senses the wireless channel before transmitting a frame. If the node detects the channel idle for a predefined time of long inter-frame space, *LIFS*, then it transmits the frame immediately. Otherwise, it attempts to transmit it again after some random

backoff time.

Finally, a broadcast source generates a packet $P(i)$ where i is the packet sequence number, which is used for unique identification of the packet in conjunction with the source address at each receiver's upper layer. Each node encapsulates the packet $P(i)$ with a broadcast MAC frame header for forwarding, and all its neighbors are intended receivers.

2.3 ST-BCAST

In this section, we describe each component of our scheme in detail.

2.3.1 Control signals

In ST-BCAST, two control signals are used for the receiver-triggered forwarding and cancellation: ready-to-forward (RTF) signal is used by a node to advertise the possession of a broadcast packet; forward-request (FR) signal is used by a node to request the forwarding of it. Both signals take the form of a *tone-signal*. Suppose that a node wants to advertise the possession of a broadcast packet $P(i)$. Then, it transmits a tone-signal on data subcarrier $j (= i \bmod (N_S/2))$ which is the RTF signal for $P(i)$, denoted as $\text{RTF}(i)$. Similarly, a node that requests the forwarding of $P(i)$ transmits a tone signal on data subcarrier $j' (= N_S/2 + (i \bmod (N_S/2)))$, which is the FR signal for $P(i)$, denoted as $\text{FR}(i)$. Each receiver identifies the type of a control

signal as well as the subcarrier number over which the tone-signal has been detected.

The benefit of using subcarrier-level tone-signals as control signals is that each receiver can detect the overlapped transmissions of a control signal correctly by measuring the energy level on each data subcarrier. Since the energy detection does not require any decoding procedure, each receiver can detect a control signal (i.e., a tone-signal) with high probability even when multiple nodes transmit it simultaneously in an asynchronous manner. We exploit this benefit of subcarrier-level tone-signals to reduce the communication overhead for the forwarding transaction.

Note that the number of simultaneous broadcasts in the network, which maintains one-on-one relationship between the sequence number and its corresponding subcarrier, is limited to $N_S/2$. Hence, if multiple source nodes generate different broadcast packets *at the same time*, some of them may assign a same subcarrier number for their packets, resulting in a confusion. We address this problem in subsection 2.3.5.

2.3.2 Forwarding state lists

Each node maintains two lists for forwarding state information.

Forwarding packet list (FPL)

A broadcast source puts a broadcast packet into its *FPL* indexed with its sequence number. As well, if a node receives a broadcast packet $P(i)$ after transmitting $FR(i)$, it puts the packet into its *FPL* to forward it when necessary. The broadcast packet will be held in *FPL* until the timer for that packet expires after *FPL_timeout*.

Requesting packet list (RPL)

This list contains the subcarrier numbers (i.e., after modulo operation) of broadcast packets that the node is currently waiting for reception. Note that the packet sequence number i is not known yet. When a node detects $RTF(i)$ (i.e., on subcarrier j) but it does not have the subcarrier number j in its *RPL*, it adds j to its *RPL* and transmits $FR(i)$ (i.e., on subcarrier j'). The subcarrier number j will be removed from *RPL* if the node receives a broadcast packet with sequence number i or the timer for subcarrier number j expires after *RPL_timeout*.

Note that each node maintains the state information independently. Since it does not share the information with its neighbors, there is no additional communication overhead except for using the two control signals $RTF(i)$ and $FR(i)$.

2.3.3 Receiver-triggered forwarding decision and cancellation

Suppose that source node s disseminates a broadcast packet $P(i)$. Then, ST-BCAST works as follows.

1. Source node s adds the packet $P(i)$ to its FPL . After that, node s transmits $RTF(i)$ as it already has the packet.
2. If a node detects $RTF(i)$ but the subcarrier number j is not in its RPL , it transmits $FR(i)$ after a predefined short interval (short inter-frame space, $SIFS$)¹ and adds j to its RPL . If the node detects $RTF(i)$ from another $RTF(i)$ sender again, it transmits $FR(i)$ after $SIFS$ and resets the timer for the subcarrier number j since it can receive the packet $P(i)$ from that $RTF(i)$ sender.
3. If a node detects $FR(i)$ and has the packet $P(i)$ in its FPL , it forwards the packet after a random backoff time $T_{backoff} \in [0, T_{max}]$. While the node is waiting for its transmission, if it detects $RTF(i)$ before the backoff timer expires, it cancels its scheduled transmission for the packet.
4. If a node receives the packet $P(i)$ which corresponds to the subcarrier number j in its RPL , it transmits $RTF(i)$ after $SIFS$, and removes j from its RPL . Then, it adds the packet $P(i)$ to its FPL .

¹Note that $SIFS$ is shorter than $LIFS$ defined in Section 2.2.

5. If a node cannot receive any broadcast packet with a sequence number i after transmitting $\text{FR}(i)$ within FR_tx_interval , it retransmits $\text{FR}(i)$. If the number of retransmissions reaches a predefined number, it removes the subcarrier number j from its RPL and gives up the packet.

From steps 2 and 3, a node that has a broadcast packet $P(i)$ forwards the packet *only if* there is an explicit request for the packet, i.e., on the reception of $\text{FR}(i)$. This receiver-triggered forwarding decision prevents unnecessary transmissions of the packet. Furthermore, the forwarding cancellation mechanism, which makes $\text{FR}(i)$ receivers cancel their transmission schedules of the packet $P(i)$ after detecting $\text{RTF}(i)$ (i.e., reception of the packet $P(i)$), reduces the number of redundant transmissions further.

What happens if a node cancels the transmission when some of its neighbors have not received $P(i)$ yet? These neighbors will keep retransmitting $\text{FR}(i)$ according to step 5, prompting their neighbors to reschedule the transmission of it. Therefore, the forwarding cancellation after receiving $\text{RTF}(i)$ does not harm reliable broadcasting.

We highlight that the transaction of $P(i)$ - $\text{RTF}(i)$ - $\text{FR}(i)$ can be completed without any interruption from data transmissions of other nodes. In Section 2.2, we assume that a node can transmit a data frame on the wireless channel only if it can detect an idle channel for LIFS , that is much longer than SIFS . Since new $P(i)$ receivers transmit $\text{RTF}(i)$ after SIFS of $P(i)$ reception and corresponding

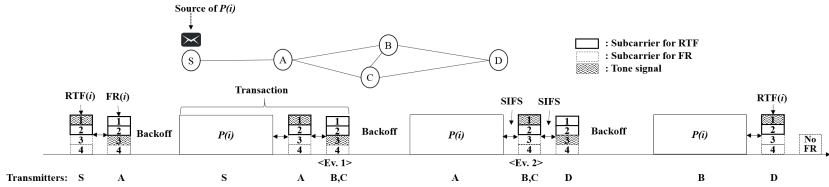


Figure 2.1: An example of protocol operation when node S wants to flood a broadcast packet $P(i)$. In this example, the number of available subcarriers is 4.

$P(i)$ requesters transmit $FR(i)$ after $SIFS$ of $RTF(i)$ reception, other nodes that are not involved in the transaction for $P(i)$ cannot detect an idle channel for $LIFS$, resulting in the re-initialization of their backoff.

Finally, multiple neighbor nodes can transmit a control signal for the same packet concurrently in ST-BCAST. According to step 2, nodes that receive $RTF(i)$ will transmit $FR(i)$ simultaneously. Similarly, according to step 4, nodes that receive a broadcast packet $P(i)$ will transmit $RTF(i)$ concurrently if they receive the packet at the same time. However, these overlapped transmissions of the control signals can be identified by receivers correctly thanks to the benefit of designing control signals as simple subcarrier-level tone-signals.

2.3.4 Operation example

Fig.2.1 depicts an example of protocol operation when we adopt *subcarrier-level tone-signals* as control signals. In this example, the source has a packet $P(i)$ to broadcast, and N_S is 4. First, the source node S

transmits a tone-signal of $\text{RTF}(i)$ to advertise the presence of $P(i)$ on subcarrier 1, assuming that $i \bmod (N_S/2) = 1$. Then, node A detects $\text{RTF}(i)$ on subcarrier 1 and responds with $\text{FR}(i)$ on subcarrier 3 ($= N_S/2 + i \bmod (N_S/2)$). Node S detects $\text{FR}(i)$ and decides to transmit $P(i)$ after a random backoff time.

Suppose that node A has received $P(i)$ successfully. Then, node A responds with $\text{RTF}(i)$. Nodes B and C receive $\text{RTF}(i)$ at the same time, and thus transmit $\text{FR}(i)$ simultaneously (see <Ev.1> in Fig.2.1 where ‘Ev’ represents an event). Though the two signals overlap, node A can figure out $\text{FR}(i)$ since it observes an energy peak only on subcarrier 3. Now, node A decides to forward $P(i)$ after some backoff time. Then, nodes B and C respond with $\text{RTF}(i)$ at the same time after receiving $P(i)$ (<Ev.2> in Fig.2.1). In this case, node D recognizes $\text{RTF}(i)$ by detecting an energy peak only on subcarrier 1, and responds with $\text{FR}(i)$ making nodes B and C schedule the transmission of $P(i)$.

Finally, suppose that node B picks up a smaller backoff time than node C . Then, node B transmits $P(i)$, which is followed by $\text{RTF}(i)$ from node D , and node C will cancel its transmission according to step 3. After that, the broadcast of $P(i)$ ends since any node will not transmit $\text{FR}(i)$.

2.3.5 Mode switching mechanism for multiple source case

Using *subcarrier-level tone-signals* for control signals makes the additional communication overhead for exchanging *RTF* and *FR* constant by allowing control signal transmissions to overlap. However, as mentioned in subsection 2.3.1, the limitation on the number of data subcarriers can cause a problem when multiple sources generate different broadcast packets *at the same time*, and some of them use a same subcarrier number for their packets. The broadcasts with the same subcarrier number j can cause a confusion at intermediate nodes, resulting in incomplete broadcast.

To alleviate this problem, we propose a simple mode switching mechanism. Suppose that two different source nodes v and w happen to broadcast their packets, denoted as $P_v(i)$ and $P_w(i')$, at the same time. If $i \bmod (N_S/2)$ is equal to $i' \bmod (N_S/2)$, both sources will assign a same subcarrier number j to their packets, which will be broadcasted using the same control signals, $\text{RTF}(i)$ and $\text{FR}(i)$. Therefore, if an intermediate node x detects $\text{RTF}(i)$, it will transmit $\text{FR}(i)$, and delete j from its *RPL* if it receives either $P_v(i)$ or $P_w(i')$.

Let us consider that node x has received $P_v(i)$ first. Then, it is possible for node x to receive $P_w(i')$ from one of its neighbors even though node x has not transmitted $\text{FR}(i')$ for $P_w(i')$ ². In this case,

²A neighbor that transmits $P_w(i')$ will have another neighbor that has transmitted $\text{FR}(i')$ for $P_w(i')$.

node x checks at its upper layer whether it has already received a broadcast packet with the sequence number i' from the source w . If not, node x sets a bit-flag ‘treat-as-flooding’ in its MAC header and broadcasts it following the conventional flooding, i.e., forwards the packet after some random backoff time without any tone-signals. Any node that receives a broadcast packet with the ‘treat-as-flooding’ flag performs the same operation as node x . In other words, $P_w(i')$ will be broadcasted following the conventional flooding when the duplicate use of a subcarrier number has been detected.

2.3.6 Physical layer aspects for RTF and FR transmission and detection

With respect to the practical implementation of ST-BCAST, there are two major challenges on tone-signal based operation: the presence of frequency-selective noise and the mismatch between tone-signal transmission range and data transmission range. We address these challenges by using higher transmission power and energy detection threshold for tone-signal transmission and detection, respectively. Intuitively, using high level of detection threshold reduces the false alarms of tone-signal presence under frequency-selective noise. Then, we can tune the transmission power of the tone signal to make the tone signal transmission range and the data transmission range be identical through empirical measurements.

2.3.7 Duration of RTF and FR

When a node senses a transmission on the channel, it performs FFT using the received time-domain samples to extract spectral components. If the transmitted signal is a tone-signal, the node can identify the subcarrier number over which the tone-signal has been transmitted, by calculating the magnitude of the extracted spectral components. However, for the successful detection of a tone-signal, all the time-domain samples fed into FFT block (i.e., N_{FFT} samples in total) should contain tone-signal information [34]. Therefore, the duration of RTF and FR should be greater than N_{FFT}/W that denotes the duration of an OFDM symbol without cyclic prefix [61]. We conjecture that setting the duration of control signals as a multiple of N_{FFT}/W would be sufficient for robust detection.

2.4 Reliability of ST-BCAST

In this section, we analyze the reliability of ST-BCAST. First, we introduce two conditions for reliable broadcast and show that the two conditions are sufficient for guaranteeing the complete delivery of a broadcast packet to all nodes in the network. Then, we show that ST-BCAST satisfies the two conditions assuming that RTF signals are detected without errors.

Notations and assumptions used in the analysis are as follows. We consider a wireless multi-hop network that is represented by a graph

$G(V, E)$ where V is the set of nodes and E is the set of edges. The graph G is a connected graph, i.e., any node $v, w \in V$ can communicate with each other through a direct link or multi-hop routes. We assume that a source node s begins to broadcast a packet $P(i)$. We represent the set of l -hop neighbors of node $v \in V$ as $N_l(v)$.

First-hop delivery condition. *Suppose that the source node $s \in V$ transmits $P(i)$. Then, all nodes in $N_1(s)$ receive $P(i)$.*

Successful relay condition. *Consider node $v \in V$ that has not received $P(i)$ yet. If any node $w \in N_1(v)$ receives $P(i)$, then node v receives $P(i)$ eventually.*

The two conditions are sufficient for the completion of the broadcast for $P(i)$.

Proposition 1. *Suppose node s begins to broadcast $P(i)$. If first-hop delivery condition and successful relay condition are true, then all nodes in $V \setminus s$ receive $P(i)$.*

Proof. Let the maximum hop distance between node s and another node $w \in V \setminus s$ be L . We denote the entire set V as

$$V = \{s, N_1(s), N_2(s), \dots, N_L(s)\}. \quad (2.2)$$

We use the mathematical induction to show that every node in $N_l(v)$ where $l \in \{1, 2, \dots, L\}$ receives $P(i)$. First, all nodes in $N_1(s)$ receive $P(i)$ since first-hop delivery condition is true. Suppose that all nodes

in $N_k(s)$ receive $P(i)$ where $1 \leq k \leq L-1, k \in \mathbb{N}$. Note that any node $x \in N_{k+1}(s)$ has at least one connected neighboring node in $N_k(s)$. Since we assume that all nodes in $N_k(s)$ have received $P(i)$, all nodes in $N_{k+1}(s)$ receive $P(i)$ by successful relay condition. Therefore, first-hop delivery condition and successful relay condition are sufficient conditions for delivering $P(i)$ to all the nodes in $V \setminus s$. \square

Proposition 1 implies that any broadcast protocol that satisfies first-hop delivery condition and successful relay condition guarantees the reliable delivery of $P(i)$ over the network. ST-BCAST satisfies the two conditions if the transmission of $RTF(i)$ is correctly detected by neighboring nodes.

Claim 1. *Let node s be the source of broadcast packet $P(i)$. If each node detects the transmission of $RTF(i)$ correctly (and $FR(i)$ with non-zero probability), then ST-BCAST satisfies first-hop delivery condition and successful relay condition.*

Proof. First, we prove that ST-BCAST satisfies first-hop delivery condition. When node s transmits $RTF(i)$, all nodes in $N_1(s)$ detect $RTF(i)$ by the assumption. Thus, they add the subcarrier number $j(= i \bmod (N_S/2))$ to their $RPLs$ and transmit $FR(i)$. If node s detects $FR(i)$, then it transmits $P(i)$ after some backoff time. If node s fails to detect $FR(i)$, nodes in $N_1(s)$ will transmit $FR(i)$ again, making node s forward $P(i)$.

Suppose that node s transmits $P(i)$ after detecting $FR(i)$ from

its neighbors in $N_1(s)$. If all nodes in $N_1(s)$ receive $P(i)$, then they stop transmitting $\text{FR}(i)$ and first-hop delivery condition holds. Otherwise, some nodes in $N_1(s)$ that have not received $P(i)$ transmit $\text{FR}(i)$ periodically until they receive $P(i)$. Since node s schedules the transmission of $P(i)$ whenever it detects $\text{FR}(i)$, all nodes in $N_1(s)$ can receive $P(i)$ eventually.

We now prove that ST-BCAST satisfies successful relay condition. Suppose that a certain node $v \in V \setminus s$ has not received $P(i)$. If node $w \in N_1(v)$ receives $P(i)$ for the first time, it transmits $\text{RTF}(i)$. Then we treat node w as a new source node of $P(i)$ that has transmitted $\text{RTF}(i)$. Since node v belongs to $N_1(w)$, it receives $P(i)$ by first-hop delivery condition. Therefore, ST-BCAST satisfies successful relay condition, which completes the proof. \square

Previous feedback-based broadcast protocols that use the information of neighboring nodes can also satisfy the two conditions. However, they often consume a significant amount of communication resource to check per-neighbor feedback messages. For counter-based and probability-based protocols, the two conditions are not satisfied even when there is neither a channel error nor a collision, since a node that is essential for network connectivity may not forward the received packet.

In practical wireless multi-hop networks, Claim 1 may not be always true since $\text{RTF}(i)$ can be lost for some reasons such as channel distortion. However, detecting $\text{RTF}(i)$ will be more robust to channel

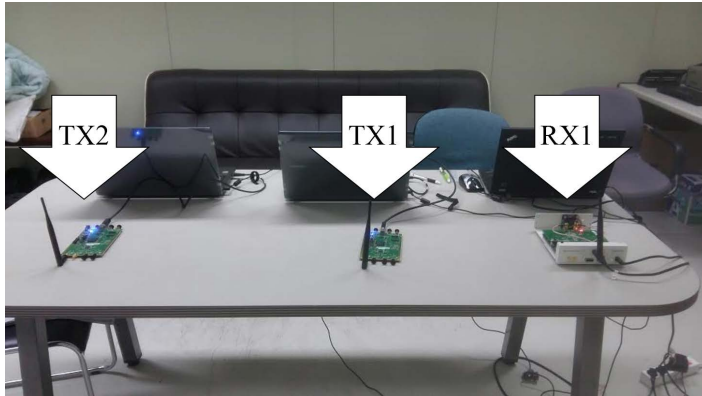


Figure 2.2: The testbed consisting of three USRP hosts. The right most host acts as a tone-signal detector (RX1). The other two hosts (TX1, TX2) act as tone-signal transmitters.

fading and collisions than receiving $P(i)$ directly, thanks to the energy detection technique. Additionally, there can be multiple chances for a node to receive $\text{RTF}(i)$ if its neighboring nodes receive $P(i)$ at different times, increasing the probability of recognizing $P(i)$. Once a node recognizes the presence of $P(i)$ by detecting $\text{RTF}(i)$, it transmits $\text{FR}(i)$ until it receives $P(i)$.

2.5 Feasibility of tone signal detection

In this section, we confirm the feasibility of tone-signal generation and detection through experiments using USRP devices and GNU Radio software package [63]. We set up a simple testbed that consists of three hosts as shown in Fig. 2.2. One host acts as a tone-signal detector (RX1), and the other two hosts act as tone-signal transmitters

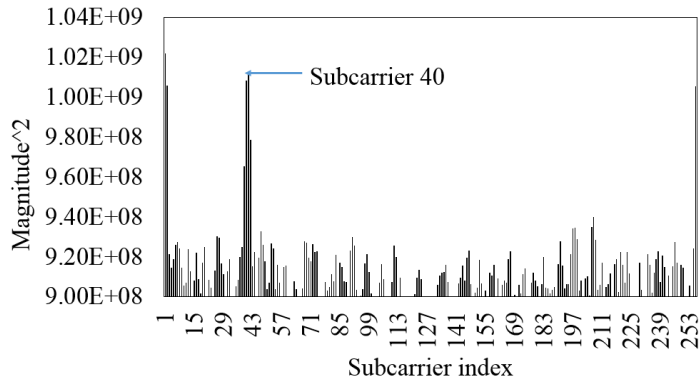


Figure 2.3: The squared magnitude of frequency-domain samples calculated at RX1 when TX1 transmits a tone-signal on subcarrier 40. We can see that there is a peak near 40th subcarrier.

(TX1, TX2). We consider an OFDM communication channel with 1 MHz baseband and 256 subcarriers. Thus, the frequency spacing between two adjacent subcarriers is 3906.25 Hz. The tone-signal detector (RX1) calculates the squared magnitude of frequency-domain samples, obtained from FFT with the time-domain complex samples.

Fig. 2.3 shows the squared magnitude of frequency-domain samples at RX1 when TX1 transmits a tone-signal on subcarrier 40. We observe that there is a peak around the subcarrier 40 as we expected. Subcarriers 0 and 255 also show peaks, but this is due to DC bias [34]. However, the adjacent subcarriers near the subcarrier 40 also show large values. This spectral leakage is known to be inevitable in practice since the time-domain samples of the observed signal is likely to contain any discontinuity at the end of the measurement time [43, 61]. Therefore, mapping a sequence number into a group of subcarriers can

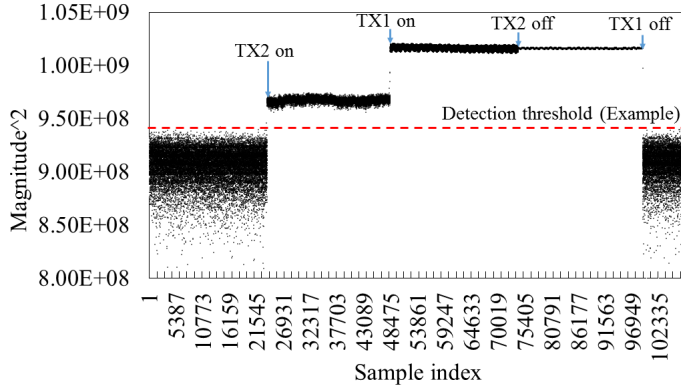


Figure 2.4: The change of the squared magnitude of frequency-domain samples on the subcarrier 40. For each point, 256 time-domain samples are fed into FFT calculator.

improve the accuracy of *RTF* and *FR* detection.

Next, we evaluate the impact of overlapped tone-signals on detection capability. Fig. 2.4 shows the change of the squared magnitude of frequency-domain samples on subcarrier 40. Note that TX1 is closer to RX1 than TX2. First, only noise exists when both transmitters are inactive. When TX2 begins to transmit a tone-signal on subcarrier 40, values on that subcarrier increase suddenly. Since the values are greater than the detection threshold (the dotted red line in Fig. 2.4), RX1 can decide that a tone-signal has been transmitted on the subcarrier 40. After that, TX1 starts to transmit a tone-signal on the same subcarrier. We can see that the values increase further and do not decrease even when TX2 stops the transmission. Therefore, we claim that it is possible for a node to detect overlapped transmissions of a tone-signal by measuring the energy of spectral components, and

the received signal strength is dominated by the transmission from a node that is close to the receiver.

However, the overlapping feature of the control signals may cause a side effect, since the multiple simultaneous transmissions of a control signal can increase their transmission range. As we noted, the mismatch of transmission ranges of *RTF* and *FR* signals can lead to undesirable forwarding behavior. Hence, the dynamic control of transmission power for the signals to achieve consistent transmission range remains as an interesting open problem.

2.6 Simulation results

In this section, we evaluate the performance of ST-BCAST through simulations. We implemented ST-BCAST on NS-3 network simulator, and compared it with other broadcast schemes that operate without topological information: unconditional flooding, GOSSIP1(p), and GOSSIP3(p, k, m) [44]. The simulation results show that ST-BCAST outperforms the others in both reliability and efficiency.

2.6.1 Implementation

We implemented ST-BCAST by modifying WiFi modules provided in NS-3.21 package [64]. We added ready-to-forward and forward-request signals to the set of MAC-layer control frames. A node can detect these signals if the received power is higher than *RTF* detec-

Table 2.1: Simulation parameters used for ST-BCAST

Parameter	Value
Energy detection threshold for CCA	-96.0 (dBm)
RTF detection threshold (RTF_thres)	-95.2 (dBm)
FR detection threshold (FR_thres)	-94.4 (dBm)
Forwarding packet list timeout ($FPL_timeout$)	600 (msec)
Requesting packet list timeout ($RPL_timeout$)	300 (msec)
FR transmission interval ($FR_tx_interval$)	50 (msec)
Duration of RTF (T_{RTF})	10 (μ sec)
Duration of FR (T_{FR})	10 (μ sec)
Duration of $SIFS$	9 (μ sec)
Duration of $LIFS$	34 (μ sec)
Number of data subcarriers (N_S)	48

tion threshold (RTF_thres) and FR detection threshold (FR_thres), respectively. We set the energy detection threshold, RTF_thres , and FR_thres as -96 dBm, -95.2 dBm, -94.4 dBm, respectively. Setting FR_thres slightly higher than RTF_thres helps nodes that have weak links with FR transmitters to avoid unreliable packet forwarding. The simulation parameters for ST-BCAST are listed in Table. 2.1.

2.6.2 Broadcast schemes in comparison

We compared ST-BCAST with the other three well-known broadcast schemes: flooding, GOSSIP1(p), and GOSSIP3(p, k, m). In the flooding scheme, if a node receives a broadcast packet, it forwards the packet after a random backoff time. In GOSSIP1(p), if a node receives the packet, then it forwards the packet after a random backoff time with probability p . GOSSIP3(p, k, m) adds some forwarding condi-

tions to GOSSIP1(p) in order to improve the coverage of broadcast. In GOSSIP3(p, k, m), nodes within the first k -hop from the source node forward the packet with probability 1 if they receive the packet. The other nodes forward the packet with probability p or listen to the channel for a timeout period, T_{WAIT} . If they cannot overhear the transmission of the packet more than m times within T_{WAIT} , they forward the received packet with probability 1. Note that all the schemes including ours do not require any topological information. We set the parameters of p, k, m to 0.7, 1, 1, respectively, as in [44]. GOSSIP1(p) and GOSSIP3(p, k, m) are widely used in broadcast[45], and shown to achieve good performance through simulations and real testbeds[38].

2.6.3 Performance metrics

We use three performance metrics to evaluate the considered protocols.

Packet delivery ratio (PDR)

The PDR is the ratio of the number of nodes that actually received the broadcast packet to the total number of nodes that can receive the packet (i.e., connected with the source node). We consider that nodes $v, w \in V$ establish a link $l(v, w)$ if the RSP between them is larger than 0.25. Therefore, some nodes may be disconnected from the network due to poor wireless link and will be excluded when counting the total number of connected nodes.

Communication overhead (CO)

We define CO as the total sum of transmission times used for packet forwarding and signaling. Let T_P denote the transmission time for a broadcast packet, N_P denote the total number of transmissions for a broadcast packet over the network, and N_{FR} denote the total number of FR retransmissions for a packet. The overhead of all the comparable broadcast schemes can be calculated as $T_P N_P$. On the other hand, ST-BCAST consumes additional times for RTF and FR transmissions, which are denoted as T_{RTF} and T_{FR} , respectively. The CO of ST-BCAST can be obtained by calculating $(T_P + SIFS + T_{RTF} + SIFS + T_{FR})N_P + T_{FR}N_{FR}$.

Packet delivery time (PDT)

The PDT is measured as follows. Let $t_s^{P(i)}$ denote the time when source node s begins to broadcast packet $P(i)$. Suppose that node v receives $P(i)$ at time $t_v^{P(i)}$. Then, the PDT of node v for $P(i)$ is $t_v^{P(i)} - t_s^{P(i)}$.

2.6.4 Simulation environments

We use the standard 802.11 DCF for the MAC protocol [60]. Each node transmits with the same rate (6 Mbps) and power (16.0206 dBm). The size of a broadcast packet is 64 bytes. In order to model packet losses at a link that conforms to the graded SINR model, we adopt log-distance propagation loss model, constant propagation de-

lay model, and Nist error rate model [56] with default values defined in NS-3. Under these models, if a node detects a signal which strength is greater than the energy detection threshold (-96 dBm), it calculates the RSP, p_{rsp} , based on the received SINR. Then, it sends the received packet to the upper layer with the probability p_{rsp} . In the simulation, without interference, the p_{rsp} of a link is 1 if the distance between two nodes is smaller than 100 m, and decreases to 0 as the distance increases.

We consider two simulation scenarios: 1) single broadcast source, 2) multiple broadcast sources. In the first scenario, a randomly chosen source node broadcasts 5 packets at a rate of 1 packet/second. In the second scenario, multiple source nodes broadcast 5 packets *simultaneously* at the same rate. The simulation stops when there is no node in the network with the transmission schedule of the last broadcast packet. In each simulation, nodes are randomly distributed within a $1000 \times 1000 \text{ m}^2$ area. We set the backoff window size, T_{max} , to 100 ms^3 . Finally, we ran 30 simulations for each case with different random seeds. The simulation results are averaged to get a bar or point in graphs, where error bars in the graphs represent the standard error.

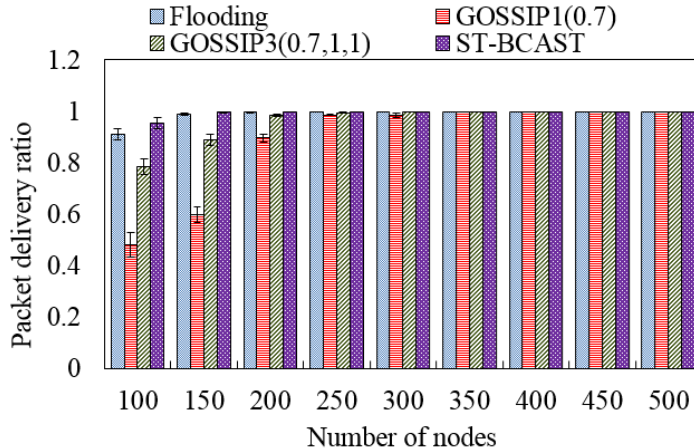


Figure 2.5: Single source - Packet delivery ratio with different node density

2.6.5 Results - single source

Fig. 2.5 shows the average PDR according to different node densities. In networks with high node density (i.e., $|V| > 250$), all the schemes achieve the PDR close to 1 since a majority of nodes participate in packet forwarding and redundant forwarding trials compensate for packet losses due to collisions or channel errors. However, as the network becomes sparser, ST-BCAST shows better PDR than the other broadcast schemes. As the degree of connectivity becomes smaller, the number of nodes that are essential for reliable packet delivery increases and losses in packet forwarding are likely to impair the PDR. In GOSSIP1(0.7) and GOSSIP3(0.7, 1, 1), a node rejects to forward a

³We may need to consider the node density for determining T_{max} . However, we use this value in all the simulations since 100 ms is enough to restrict the collision rate below an acceptable level in considered simulation scenarios.

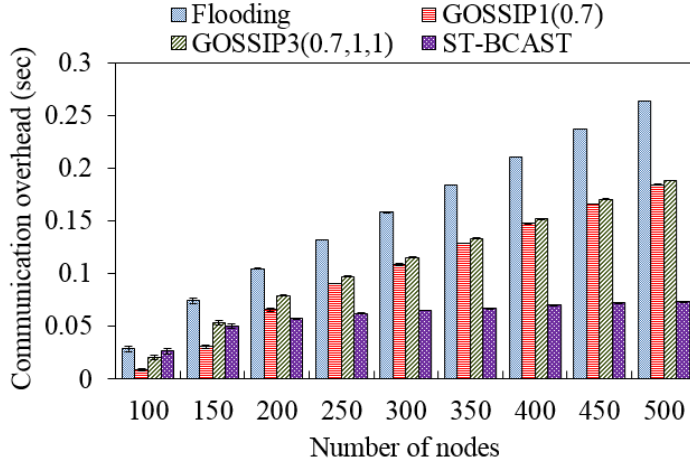


Figure 2.6: Single source - Communication overhead with different node density

received packet with probability 0.3. Hence, additional PDR drops are observed compared to the flooding scheme. In contrast, ST-BCAST suffers less packet losses, in part, because a node that has not received a packet $P(i)$ transmits $FR(i)$ repeatedly once it detects $RTF(i)$.

The advantage of ST-BCAST is more notable in the efficiency perspective. Fig. 2.6 shows the CO according to different node densities. We can see that when the number of nodes is more than 200, ST-BCAST shows the minimum CO among the compared schemes. In sparse networks, ST-BCAST shows almost the same CO with the flooding scheme since most of forwarding attempts are essential for the complete packet delivery. As node density increases, ST-BCAST successfully manages the CO at a lower level. GOSSIP1(0.7) and GOSSIP3(0.7, 1, 1) have less CO than the flooding scheme at the cost

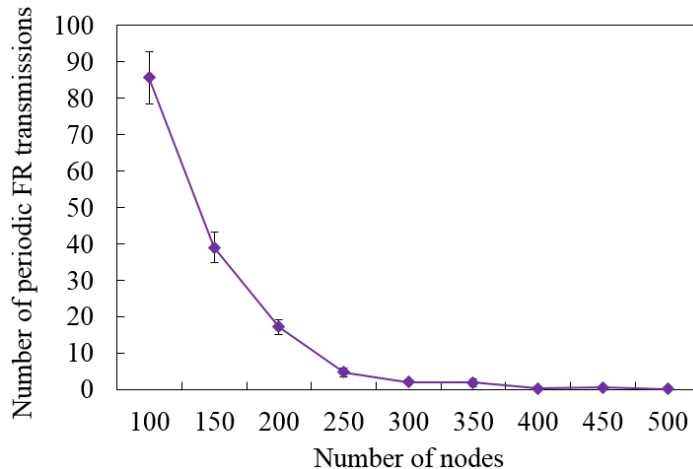


Figure 2.7: Single source - Average number of additional FR transmissions with different node density

of lowered PDR.

We emphasize that under all the other broadcast schemes, the CO increases *linearly* with respect to node density. In contrast, ST-BCAST achieves a bounded CO regardless of the node density. In ST-BCAST, the number of nodes that decide to forward a packet $P(i)$ after detecting $FR(i)$ increases as the node density increases. However, most of them cancel their transmission schedules after detecting $RTF(i)$. In addition, as shown in Fig. 2.7, the number of periodic FR transmissions also decreases as the node density increases. With higher node density, nodes have more chances of detecting $RTF(i)$, causing their periodic transmissions of $FR(i)$ to be delayed, and canceled after receiving $P(i)$.

Fig. 2.8 shows the average PDT of all the nodes in the network. We

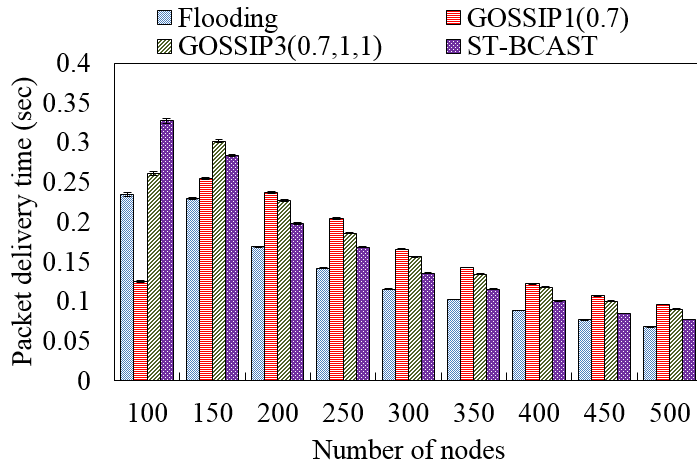


Figure 2.8: Single source - Average packet delivery time with different node density

can see that every scheme shows decreasing PDT as the node density increases. In high node density, the broadcast packet tends to be delivered through intermediate nodes over the shortest path, and the first packet forwarding tends to occur earlier because a large number of forwarding candidates schedule their transmissions after *random* backoff time within the same backoff window $[0, T_{max}]$. However, in sparse networks (100 nodes), ST-BCAST experiences larger PDT than other schemes. The reasons are two folds. First, the communication time for RTF/FR handshake is accumulated as the packet propagates. Second, ST-BCAST achieves higher PDR than the other schemes, implying that more nodes which are distant from the source node receive packets. Meanwhile, GOSSIP1(0.7) shows the low PDT in the case of 100 nodes due to its low PDR.

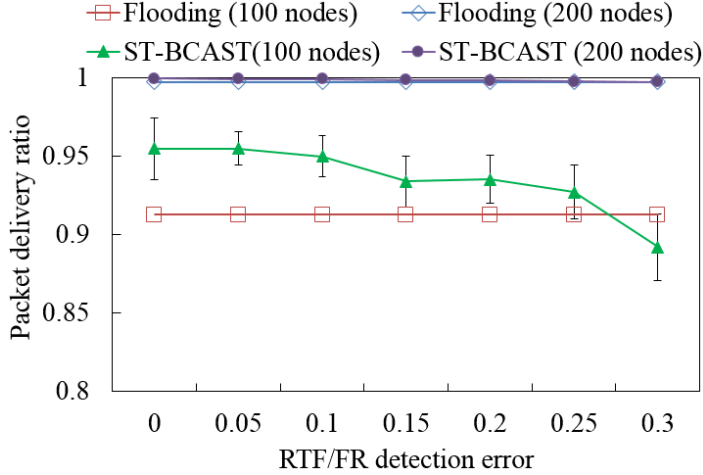


Figure 2.9: Single source - Packet delivery ratio with different signal detection error probabilities

Now, we examine the effect of signal detection errors on PDR performance. Fig. 2.9 shows the PDR of ST-BCAST according to the different detection error probabilities of RTF and FR. In sparse networks (i.e., $|V| = 100$), the detection error impairs the PDR considerably. The loss of RTF(i) hinders the nodes that have not received $P(i)$ from detecting the presence of $P(i)$. Similarly, the loss of FR(i) inhibits the essential forwarders that have received $P(i)$ from forwarding $P(i)$. However, the detection error does not affect the PDR when the node density is high (i.e., $|V| = 200$) since each node has a sufficient number of potential forwarders. Note that the PDR of ST-BCAST is still higher than that of the flooding scheme if the detection error probability is lower than 0.3.

Fig. 2.10 shows the CO of ST-BCAST according to the different

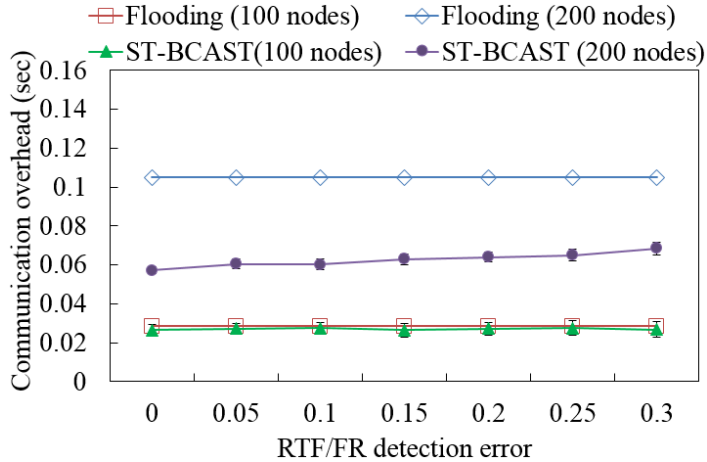


Figure 2.10: Single source - Communication overhead with different signal detection error probabilities

detection error probabilities. In the case of 100 nodes, CO does not change much with different error probabilities. However, we can see that the CO increases gradually in the case of 200 nodes. The main reason is that the detection error of $RTF(i)$ can impair the normal forwarding cancellation of a node, which results in unnecessary broadcast packet transmissions. However, the effect of signal detection error on overall CO is marginal; ST-BCAST still shows lower CO than the flooding scheme.

2.6.6 Results - multiple sources

Fig. 2.11 shows the PDR of each scheme when the total number of nodes is 200 and the number of broadcast sources is 1, 5, 10, and 15, respectively. We set the number of data subcarriers to 48. First, we can

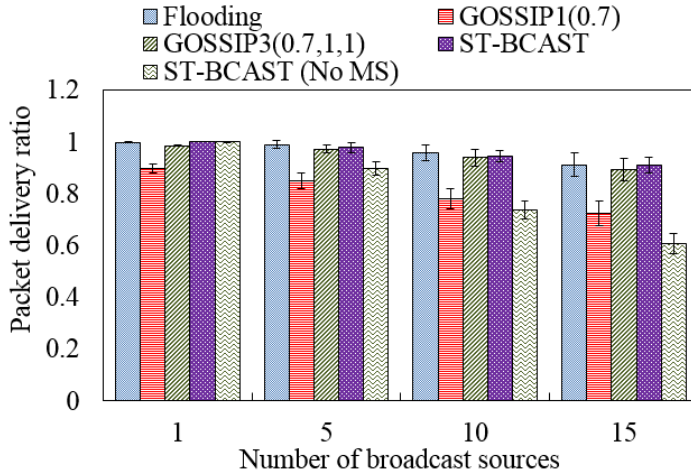


Figure 2.11: Multiple sources - Packet delivery ratio with different number of broadcast sources

see that ST-BCAST always shows comparable PDR with the flooding scheme even when multiple nodes begin to broadcast *simultaneously* thanks to the proposed simple mode switching mechanism. Without the mode switching mechanism (ST-BCAST (No MS) in the graph), the PDR drops significantly as the number of concurrent broadcast sources increases.

However, the mode switching operation increases the CO as shown in Fig. 2.12. As the number of concurrent broadcast sources increases, the sources are likely to pick up a same subcarrier number for their broadcast packets. This results in frequent packet forwarding through the conventional flooding, increasing the CO.

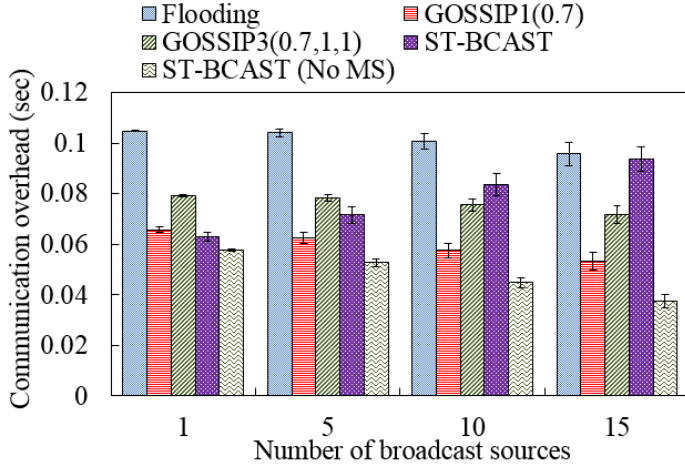


Figure 2.12: Multiple sources - Communication overhead with different number of broadcast sources

2.7 Related Work

The subcarrier-level tone-signal transmission and detection capability has been adopted in various works to improve the throughput of wireless LAN. In Back2F [43], the authors propose a frequency domain backoff mechanism where random backoff is realized by selectively transmitting a tone-signal on a subcarrier. In FICA[42], a fine-grained channel access scheme that enables subchannel-based concurrent transmissions has been proposed for improving the throughput of wireless LAN. ST-BCAST shares the benefit of subcarrier-level tone-signaling with Back2F and FICA, but ST-BCAST focuses on the reliability and scalability of broadcast, rather than throughput performance.

In SMACK [34], the authors introduce a subcarrier-level acknowl-

edgment technique for providing reliable broadcast transmission in wireless networks. In this scheme, when a node broadcasts a packet, the receivers respond with a tone-signal on the subcarrier that is associated with the packet transmitter. Then, the packet transmitter checks the presence of a tone-signal (i.e., an acknowledgment) on each subcarrier and retransmits the packet if necessary. The subcarrier-level acknowledgment has also been introduced for multicast service in wireless multi-hop networks [58]. In broadcast, the arrival times of acknowledgment tone-signals can be used to select the farthest node as the next packet forwarder, which can prevent redundant retransmissions. However, SMACK is not scalable in dense networks since every node must keep the list of its neighbors, and negotiate the acknowledgment subcarrier with all of its neighbors. In addition, nodes using SMACK should maintain 2-hop neighbor information since the next packet forwarder is determined by the current packet forwarder.

The receiver-triggered packet forwarding mechanism of ST-BCAST is motivated by the SPIN protocol which is an application-level approach for disseminating information in wireless sensor networks [26]. In SPIN, when a node obtains new data, it sends an advertisement message to its neighbors. Upon receiving the advertisement message, a neighboring node responds with a request message if it has not received the advertised data. The advertisement message sender transmits the data if it receives a request message for the advertised data.

ReMHoC [35] also takes a similar approach for reliable multicast

service in mobile ad-hoc networks. In this scheme, if a node detects the loss of a multicast packet through sequence number matching, it *multicasts* a request message that includes the sequence number for the missing data packet. If a multicast member that has the copy of the missing packet receives the request message, it responds by *multicasting* the cached copy.

The SPIN-like approach has also been adopted for disseminating emergency messages in vehicular ad-hoc networks [10]. In this scheme, the emergency message sender selects one of its neighbors as a proxy for transmitting an acknowledgment frame. When this proxy responds with an acknowledgment frame, nodes that overhear this frame transmit a request frame as 1-hop broadcast if they have not received the emergency message with the sequence number included in the acknowledgment frame.

The mentioned schemes have drawbacks for scalable broadcast. First, they require topological information (i.e., the list of neighboring nodes) for the operation. Second, they do not support concurrent transmissions of signaling messages, resulting in excessive communication overhead. In contrast, ST-BCAST requires neither any topological information nor association procedures. Furthermore, the communication overhead in the transaction of $P(i)$ -RTF(i)-FR(i) remains constant since multiple nodes can transmit RTF(i) and FR(i) simultaneously.

2.8 Summary

In this chapter, we have proposed a scalable broadcast protocol that achieves high packet delivery ratio with small communication overhead. In ST-BCAST, a node schedules the transmission of a broadcast packet only if it detects an explicit request for the packet from its neighbors. The packet transmission is delayed for a random backoff time and can be canceled in the meantime if the transmitter is notified of the packet reception from its neighbor(s). A false forwarding cancellation can be recovered by repetitive requests from the neighbors. We verified the reliability of ST-BCAST by showing that it satisfies two sufficient conditions for the complete delivery of a broadcast packet. In addition, we confirmed the feasibility of subcarrier-level tone-signaling through simple experiments using USRP devices. Finally, we showed that ST-BCAST outperforms existing broadcast schemes with respect to the reliability and efficiency through NS-3 simulation. We leave the design of a transmission power control scheme for the control signals as future work.

Chapter 3

E-GRAD: Revisiting Gradient Routing Protocol for Reliable Unicast in MANET

3.1 Introduction

Unicast transmission is a basic communication service primitive that sends a message from a single source to a single network destination identified by a unique address. Many internet applications, like file transfer, media streaming, text messaging, web surfing, use unicast transmission for delivering the contents to the destination host.

In general, unicast transmission is supported by hop-by-hop routing mechanism in MANET [46]. In hop-by-hop routing, the traffic source first finds a route to the traffic destination via the help of underlying routing protocol. The found route can consist of a single link or multiple wireless links. Then, the packet is forwarded in hop-by-hop manner through intermediate nodes on the route. The hop-by-hop routing is quite reliable and efficient if the found route does not include unreliable or congested links.

However, it is difficult for hop-by-hop routing to find and maintain a reliable route in MANET. First, there are intrinsically numerous unreliable wireless links that experience severe fluctuation in packet reception capability. At a wireless link, the received signal strength at the receiver is decreased as the distance between the transmitter and the receiver increases. In addition, it fluctuates over time due to multi-path propagation effect and Doppler spread (i.e., small-scale short-term fading) [22]. It has been known that the short-term fading in wireless communication significantly degrades the performance of hop-by-hop routing protocols [47, 55, 48].

Moreover, even through a routing protocol succeeds to find a reliable route, it can be expired in short time due to the mobility of nodes in MANET. It has been shown that the distribution of the route lifetime in typical MANET environment follows different probabilistic distribution models that shows tens of seconds in mean. The mean value decreases rapidly as the hop-count of a route increases [21]. This

limits the applicability of hop-by-hop routing in MANETs.

Gradient routing can be a good alternative approach for providing unicast service in MANET [12, 13, 49, 51]. In gradient, a source node does not find a specific route to the destination. Instead, it includes a cost value which indicates approximate distance from the destination in the packet. The cost can be calculated using hop-count, euclidean distance [50], expected energy consumption [51], signal-to-noise ratio (SNR) [13], etc. Then, intermediate nodes that receive this packet schedule the retransmission of received packet only if its cost to the packet destination is smaller than the packet transmitter. Since the multiple neighbors of a packet transmitter can participate in forwarding procedure, the gradient routing can provide a level of path diversity in unicast transmission.

In this chapter, we investigate hop-by-hop routing and gradient routing in detail, and verify that the superiority of gradient routing in reliable unicast through analysis on realistic MANET environments. Then, we propose a practical gradient forwarding architecture (E-GRAD) that uses on-demand flooding-based cost update and SNR-based cost calculation, and show that E-GRAD can achieve near upper-bound throughput under realistic environments with short-term signal fading and node mobility using NS-3 network simulator.

The rest of the paper is organized as follows. In Section 2, we explain hop-by-hop routing and gradient routing in detail. In Section 3, we verify the superiority of gradient routing over hop-by-

routing through analysis and numerical results. In Section 4, we introduce our proposed gradient forwarding architecture in detail. Section 5 provides simulation results, and we summarize this chapter in Section 6.

3.2 Forwarding mechanisms for unicast transmission

In this subsection, we introduce two representative mechanisms for unicast transmission in MANET: hop-by-hop routing and gradient routing.

3.2.1 Hop-by-hop routing

In hop-by-hop routing, the data traffic generated by a source is delivered to the destination through hop-by-hop forwarding of nodes on a route between the source and the destination. When a node on the route receives a data packet, it retransmits the received data packet to its next-hop node on the route via link-layer unicast transmission. This procedure is repeated until the data packet reaches to the destination.

In general, a routing protocol in the network layer takes the role of discovering and maintaining routes for end-to-end sessions. Many routing protocols for wireless MANETs have been developed in the literature to provide reliable unicast service efficiently [8, 5, 4, 6, 46].

In table-driven routing protocols, every node maintains a routing table which consists of per-destination routing entries. Each entry includes the next-hop information to the destination that is used for hop-by-hop forwarding. The routing table can be constructed proactively (i.e., before the generation of application traffic) [8, 5], or reactively (i.e., on the time of traffic generation) [4, 7]. In the source routing protocol [6], a traffic source includes whole route information in the header of a data packet, and every node on the route exploits this route information for hop-by-hop routing when they receive the data packet.

It has been known that hop-by-hop routing protocols achieve performance to some extent in terms of packet delivery ratio, end-to-end delay, and routing overhead if they are combined with credible link metrics, such as expected transmission counts (ETX) [52], effective number of transmissions (ENT) [53]. However, in MANET, the network topology changes dynamically over time, thus it requires significant overhead for maintaining up-to-date link metrics. In addition, the estimated value is likely to be inaccurate since the actual link quality can change while the link estimation procedure is ongoing [54]. These impairments limit the performance of hop-by-hop routing.

The more severe problem in hop-by-hop routing is the expiration of a discovered route. Suppose that a routing protocol succeeds to find a reliable route to the destination. Then, the source can deliver the packet to the destination while the links between the intermediate

node on the route are not broken. However, if any link on the route is broken, the packets on the broken link is likely to be lost, and the end-to-end packet delivery is unavailable until the routing protocol finds another reliable route to the destination. In later subsection, we show that the conventional hop-by-hop routing protocols often fail to provide reliable unicast service for end-to-end sessions even though they can be connected through reliable links in real.

To improve the reliability, we can consider maintaining multiple independent routes for each destination [14]. However, this approaches require creating and updating multiple routing path information in highly mobile environments is a challenging issue and can complicate the operation of routing protocols.

3.2.2 Gradient routing

Unlike hop-by-hop routing, nodes using gradient routing does not find a specific route to their destinations, rather they just manages cost values for each destination. The cost value represents an abstractive cost for delivering data traffic to the destination. In gradient routing, a packet transmitter appends its cost to the packet's destination in the header of data packet. Packet receivers compare the cost value in the packet with its own value, and enqueues the received packet in their transmit queue only if its cost is smaller than that in the packet. The enqueued packet is removed from the transmit queue if the node overhears a transmission of same data packet from lower-cost

node. Otherwise, the packet is transmitted after some backoff time, and the transmitter retransmits the packet if it cannot overhear the transmission of the transmitted packet from lower-cost node.

In MANETs, the cost update mechanism influences the performance of gradient routing significantly. Firstly, the cost update interval should be chosen carefully in order to balance the communication overhead and the accuracy of the cost estimation. Using small cost update interval can improve the freshness of cost information since the network topology changes over time due to the mobility of nodes. However, frequent cost update increases overall communication and processing overhead. Therefore, we have to balance the freshness of cost values and the overhead for cost update. Secondly, the number (or portion) of nodes that participate in cost update procedure should be sufficiently large in order to guarantee the path diversity of gradient forwarding. In later subsection, we show that destination-oriented hop-limited flooding based cost update can be helpful in providing reliable unicast service through gradient routing.

The type of cost used for forwarding decision is also important for maximizing the performance of gradient routing. Various types of cost has been introduced for gradient routing, such as the euclidean distance to the destination [50]¹, hop-count, signal-to-noise

¹Actually, the position information itself can be used as a cost in gradient routing. In the literatures about geographical routing protocols [50, 15, 16], nodes are assumed to know their position as well as destinations' position in the interest, and the position of packet transmitter is embedded in the packet header. Therefore, packet receivers make a decision for forwarding by comparing its own

ratio (SNR) [13], expected energy consumption [51]. In later subsection, we show that SNR-based cost allocation yields good packet delivery ratio and throughput performance using reasonable amount of wireless resources under realistic MANET environments.

3.3 Reliability analysis of hop-by-hop routing and gradient routing

In this subsection, we analyze the reliability of hop-by-hop routing and gradient routing considering practical challenges in realistic MANET environments: unreliable links and node mobility. The conceptual difference between hop-by-hop routing and gradient routing on unicast transmission is the difference in the set of intermediate nodes that participate in packet forwarding. In hop-by-hop routing, the forwarding participants form a *linear route* that consists of sequence of intermediate nodes between a source node and a destination node. On the other hand, the forwarding participants in gradient forwarding has the structure of a *forwarding mesh* that has more number of nodes than a linear route in general. This difference affects the reliability on unicast transmission significantly.

distance to the packet destination and the packet transmitter's distance to the packet destination.

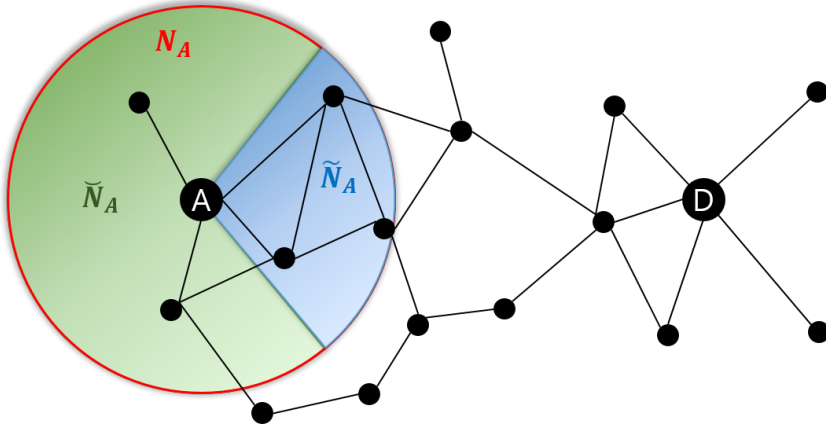


Figure 3.1: An example scenario where node A is trying to forward a packet destined to node D through gradient forwarding.

3.3.1 Impact of errors in link quality estimation

Suppose that a source node wants to deliver a data packet to a destination node. In hop-by-hop routing, the routing protocol tries to discover a route to the destination in proactive or reactive manner. And by chance, let us assume that an unreliable link has been included on the discovered route. This may be possible due to the inaccuracies in link quality estimation or link connectivity check. In this case, the reliability of unicast transmission will be significantly deteriorated due to frequent retransmissions or packet losses on the unreliable link. The chance of including an unreliable link may increase as the distance between the source and the destination increases.

However, the reliability of unicast transmission in gradient routing does not severely affected by inaccuracies in link quality estimation or link connectivity check under moderate node density thanks to the

diversity effect on packet forwarding. Fig. 3.1 describes an example scenario where node A is trying to forward a received packet destined to node D through gradient forwarding. Here, N_A is the set of neighbors of node A , \tilde{N}_A is the subset of nodes in N_A that are closer than node A from node D , and $\check{N}_A = N_A \setminus \tilde{N}_A$ is the subset of nodes in N_A that are farther than node A from node D . In gradient routing, the packet forwarding can continue if at least a single node in \tilde{N}_A has smaller cost than node A . In the other words, even though some of nodes in \tilde{N}_A have larger cost than node A due to the misbehavior in cost update procedure, node A 's transmission can be received by other nodes in \tilde{N}_A with correct (i.e., smaller) cost to node D , and they will rebroadcast the received packet after random backoff time.

Of course, invalid packet forwarding cancellation can occur if some of nodes in \check{N}_A has smaller cost than node A , and one of them transmits the received packet from node A more earlier than correct forwarding candidates in \tilde{N}_A . However, the nodes in \tilde{N}_A are likely to be hidden from nodes in \check{N}_A , resulting in the correct retransmission of the received packet. In addition, the forwarding procedure can continue even though a node in \check{N}_A transmits the received packet first if it has valid another neighboring nodes that are connected to node D . In subsection 3.5, we show that the packet delivery ratio is kept high even with the events of invalid packet forwarding cancellation.

3.3.2 Impact of node mobility

Now, we analyze the effect of node mobility on the reliability of unicast transmissions in hop-by-hop routing and gradient routing. The main idea of the analysis is to investigate the lifetime of a *linear route* in hop-by-hop routing, and the lifetime of a *forwarding mesh* in gradient routing.

First, we assume that the location of nodes and the cost values to destinations are given to hop-by-hop routing protocol and gradient routing protocol. And let us consider that the hop-by-hop routing protocol succeeds to find a route between a source v_1 and a destination v_k that consists of $k - 2$ number of intermediate nodes. Then, we can represent the found linear route R_{v_1, v_k} as

$$R_{v_1, v_k} = \{v_1, v_2, v_3, \dots, v_{k-1}, v_k\}. \quad (3.1)$$

Second, we can define the lifetime of R_{v_1, v_k} as the length of the longest time interval $[t_1, t_2]$, during which each of $k - 1$ links are kept connected [21]. Since the route is considered as disconnected if at least one of the $k - 1$ links does not exist, the lifetime of the route is limited by the lifetime of a link on the route with minimum lifetime. Therefore, if we denote the lifetime of a link $l_{v, w}$, $v, w \in V$ as $LT_{l_{v, w}}$, the lifetime of a linear route R_{v_1, v_k} , $LT_{R_{v_1, v_k}}$, can be represented as

$$LT_{R_{v_1, v_k}} = \min_{1 \leq i < k} LT_{l_{v_i, v_{i+1}}}. \quad (3.2)$$

Third, let us consider that a forwarding mesh between v_1 and v_k , F_{v_1, v_k} , has been constructed through cost update procedure in gradient routing. Then, we define the lifetime of F_{v_1, v_k} , $LT_{F_{v_1, v_k}}$, as the duration that a packet can be forwarded from v_1 to v_k through the forwarding mechanism of gradient routing.

Then, the following claim reveals the superiority of gradient forwarding against hop-by-hop routing on the reliability of unicast transmission in mobile environments.

Claim 2. *Suppose that a forwarding mesh between v_1 and v_k , F_{v_1, v_k} , consists of a set of linear routes between v_1 and v_k , denoted as $\mathcal{R}_{F_{v_1, v_k}}$. And a linear route between v_1 and v_k found by hop-by-hop routing protocol, R_{v_1, v_k} , belongs to $\mathcal{R}_{F_{v_1, v_k}}$. Then, the lifetime of F_{v_1, v_k} , $LT_{F_{v_1, v_k}}$ is always greater than or equal to $LT_{R_{v_1, v_k}}$.*

Proof. First, suppose that $\mathcal{R}_{F_{v_1, v_k}}$ has only one linear route R_{v_1, v_k} . Then, it is trivial that $LT_{F_{v_1, v_k}}$ is equal to $LT_{R_{v_1, v_k}}$. Second, suppose that the number of elements in $\mathcal{R}_{F_{v_1, v_k}}$ is larger than one. In this case, if R_{v_1, v_k} has the longest lifetime among all linear routes in $\mathcal{R}_{F_{v_1, v_k}}$, then it is also trivial that $LT_{F_{v_1, v_k}}$ is equal to $LT_{R_{v_1, v_k}}$. Otherwise, there is always a linear route $R^i_{v_1, v_k}$ in $\mathcal{R}_{F_{v_1, v_k}}$ that has longer lifetime than R_{v_1, v_k} . Since the packet can be forwarded through a linear route $R^i_{v_1, v_k}$, $LT_{F_{v_1, v_k}}$ is greater than $LT_{R_{v_1, v_k}}$ according to the definition of the forwarding mesh lifetime. \square

Fig. 3.2 shows an example scenario that supports Claim 2. Ac-

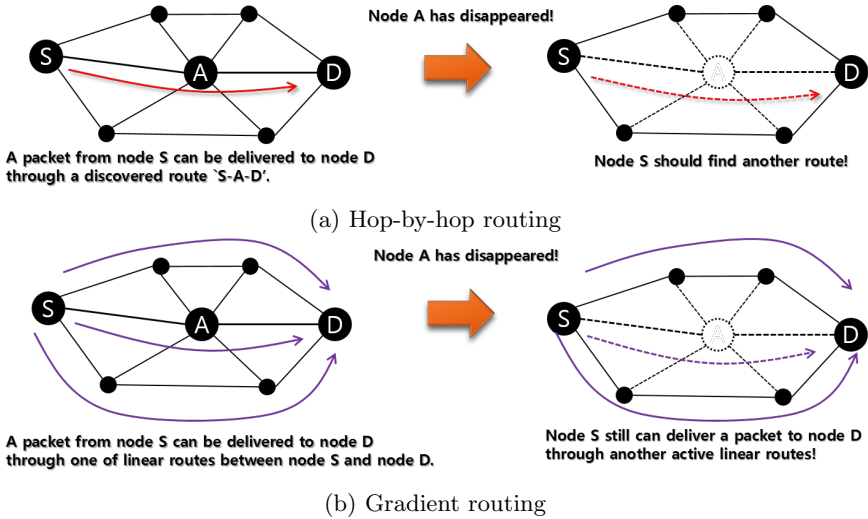


Figure 3.2: The operation of hop-by-hop routing and gradient routing when there is an active session between node S and node D. Node A moves out from the route while the session is active.

According to Fig. 3.2a, if node A on a discovered linear route (S-A-D) disappears, then the route is no longer valid and the traffic from the source cannot be delivered to node D until node S finds another route to node D. This results in packet drops at the link-layer or long delays in the application when the packet buffering is used on a broken link. However, in gradient routing, the unicast service can continue even though node A moves out since the data packet can be forwarded to node D through another live linear routes as shown in Fig. 3.2b. Note that the forwarding in the gradient routing continues without any route recovery procedures.

Type	Destination (DST)	Source (SRC)	Cost to the source (COST-TO-SRC)	Sequence number (URM-SN)
------	-------------------	--------------	----------------------------------	--------------------------

(a) Update request message (URM)

Type	Time-to-live (TTL)	Source (SRC)	Cost to the source (COST-TO-SRC)	Sequence number (UM-SN)
------	--------------------	--------------	----------------------------------	-------------------------

(b) Update message (UM)

Type	Destination (DST)	Source (SRC)
------	-------------------	--------------

(c) Update broadcast termination message (UBTM)

Figure 3.3: Signaling messages used in E-GRAD.

3.4 E-GRAD: A practical greedy routing architecture for MANET

In this subsection, we introduce a practical gradient routing architecture, named Enhanced-GRADient routing (E-GRAD), that can provide reliable unicast service under realistic MANET environments. E-GRAD consists of two major cost management components: on-demand flooding-based per-destination cost update protocol and SNR-based cost calculation function.

3.4.1 On-demand flooding-based cost update protocol

In E-GRAD, when a node has an unicast packet to send, it first checks whether it has a valid cost to the packet destination. If it has a valid cost, then it forwards the packet through gradient routing procedure as described in subsection 2.2. If not, it generates an Update request message (URM) for triggering the periodic flooding of Update message

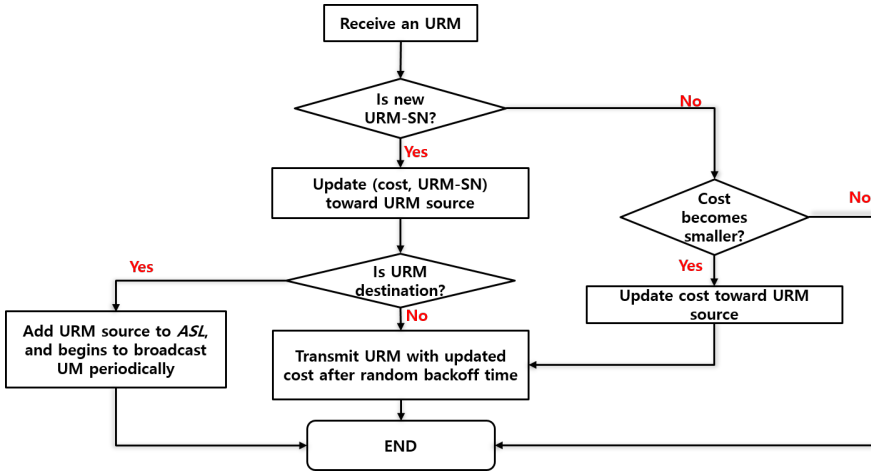


Figure 3.4: The operation flow diagram of node when it receives an URM.

(UM) from the packet destination. The structure of URM message is shown in Fig. 3.3a. The source node of URM sets the destination and the source fields in URM with the addresses of data packet destination and itself, respectively. And it sets the cost to the source field as 0. The sequence number can be allocated by the URM source randomly. Then, it broadcasts generated URM through link-layer broadcast. After that, if a non-destination node receives an URM, it first calculates its cost to the URM source, and rebroadcasts the received URM with its own cost to the URM source after random backoff time. The cost value in URM will increase as the URM propagates on the network. The sequence number field is used for checking duplicate reception of the same URM. Fig. 3.4 describes the operation flow diagram of a node when it receives an URM.

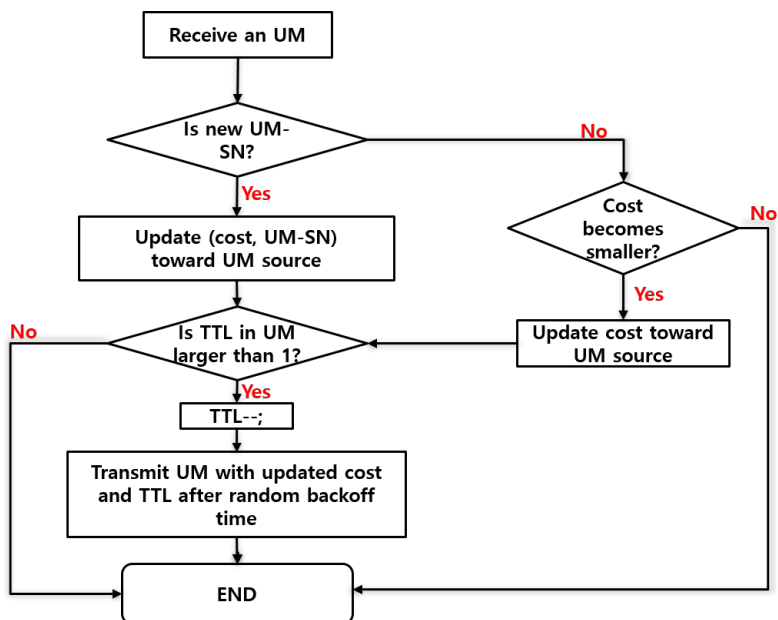


Figure 3.5: The operation flow diagram of node when it receives an UM.

Now suppose that the destination node receives the URM generated by the traffic source. Then, it adds the URM source to its *active source list (ASL)* with its cost to the URM source, and begins to broadcast UM periodically. Fig. 3.3b depicts the format of UM. The source field in UM is set as the address of UM generator, i.e., the traffic destination, and the sequence number is incremented by 1 whenever new UM is generated by the destination node. If a node receives an UM, it updates its own cost to the UM source, and re-broadcasts the received UM if the UM has higher sequence number or it has the same UM sequence number with previous UM but the cost value becomes smaller. Fig. 3.5 describes the operation flow diagram

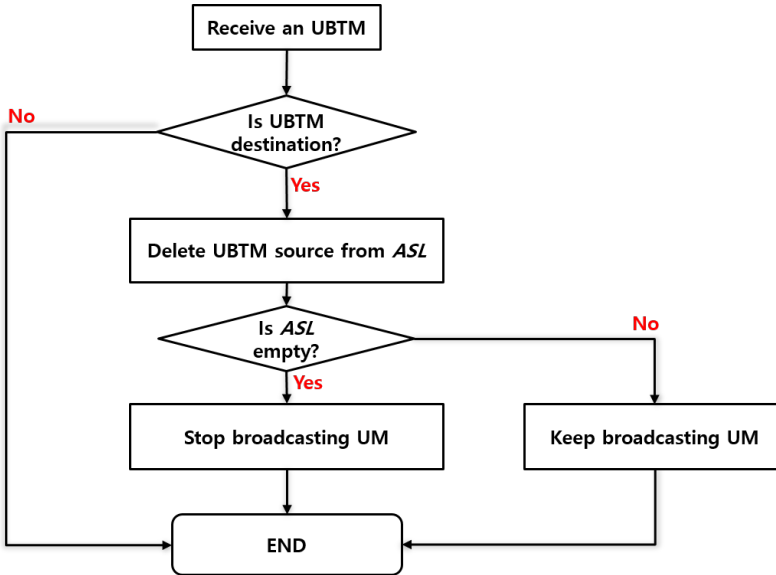


Figure 3.6: The operation flow diagram of node when it receives an UBTM.

of a node when it receives an UM.

Unlike URM, UM has a time-to-live field in the message. This field is used for controlling the cost management area where UM is required to be delivered. The destination node which has to broadcast UM periodically sets the time-to-live field in each UM as the *maximum value* of costs in its *ASL*. In the other words, the area where UM is broadcasted will be restricted to a circle where the farthest source is located at the boundary of the circle. By doing so, we can reduce the overhead for maintaining per-destination cost.

Finally, if the traffic source decides that it does not have any packet toward the traffic destination, it sends an Update broadcast termination message (UBTM) to the traffic destination which is broadcasting

UM periodically. If the destination node receives the UBTM, it deletes the UBTM source from its *ASL*, and stop to broadcast UM if its *ASL* becomes empty. The operation flow of a node when it receives an UBTM is described in Fig. 3.6.

3.4.2 SNR-based cost allocation

In E-GRAD, a node that receives an UM updates its cost toward UM source as *the sum of the cost value in UM and its perceived link cost from the UM transmitter*. The perceived link cost is calculated using the SNR value that is estimated by the physical layer during the reception of UM. If the estimated SNR value is high, i.e., larger than some threshold, then it decides that the link between itself and UM transmitter is reliable, and it sets its perceived cost as a minimum value. However, if the estimated SNR value is smaller than the threshold, it sets the perceived cost as an integer value that is inversely proportional to the estimated SNR.

More specifically, suppose that node A receives an UM that is generated by a destination node D. If the estimated SNR value, SNR_{UM} , is larger than a threshold value, SNR_{THRES} , then node A calculates its cost toward node D, C_A^D , as follows.

$$C_A^D = C_{UM}^D + 1, \quad (3.3)$$

where C_{UM}^D is the cost value of the UM transmitter. Otherwise, if

Algorithm 1 SNR-based cost allocation algorithm

Notations

- C_A^D : The cost toward node D at node A
 C_{UM}^D : The cost toward node D at UM transmitter
 SNR_{UM} : The estimated SNR value when a node receives an UM
(unit: dB)
 SNR_{THRES} : A threshold value for cost allocation (unit: dB)

Algorithm

- 1: Node A receives an UM that is originated from node D
 - 2: **if** $SNR_{UM} > SNR_{THRES}$ **then**
 - 3: $C_A^D = C_{UM}^D + 1$
 - 4: **else**
 - 5: $C_A^D = C_{UM}^D + \lceil SNR_{THRES} + 1 - SNR_{UM} \rceil$
 - 6: **end if**
-

SNR_{UM} is equal to or smaller than SNR_{THRES} , then node A calculates C_A^D as follows.

$$C_A^D = C_{UM}^D + \lceil SNR_{THRES} + 1 - SNR_{UM} \rceil. \quad (3.4)$$

The detail of SNR-based cost allocation is shown in Algorithm 1.

About the proposed cost calculation algorithm, the readers may have the following question: “In wireless communications, the SNR value experienced by a receiver fluctuates over time due to the short-term fading effect of transmitted signal. Therefore, the instantaneous SNR based cost may not reflect the typical link quality accurately. Isn’t it a problem?” Our answer is that it is not a severe problem in the gradient routing. First, as explained in subsection 2.3.1, the unicast packet can be delivered to the destination through a forward-

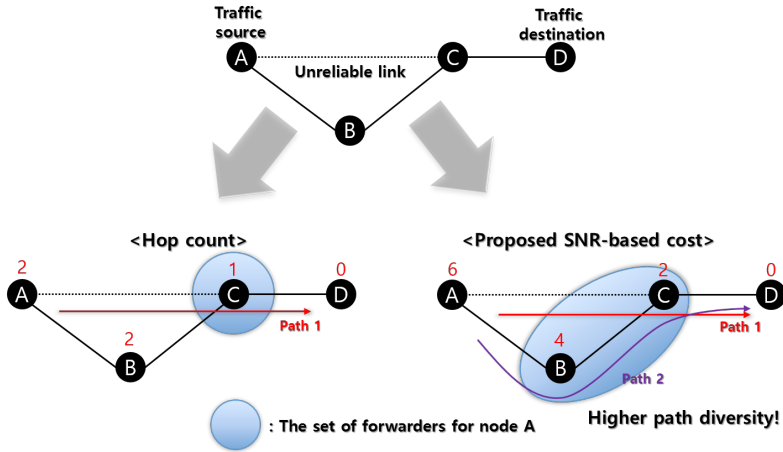


Figure 3.7: An example of MANET scenario. Node A is a traffic source, and node D is a traffic destination. In this example, the link between node A and node C is unreliable.

ing mesh if there is *at least* a linear route where costs of intermediate nodes decrease toward the destination. In the other words, the effect of fluctuation can be compensated thanks to the path diversity in gradient routing.

Second, even though short-term signal fading effect incurs a level of fluctuation on the SNR value at a receiver, the high SNR value with successful packet reception can be achieved only if the transmitted signal does not experience significant shadowing or distance-driven path loss. This is quite intuitive, and many experimental results also support above statement [17, 18]. Therefore, allocating a small cost to a node that receives UM with high SNR makes the node as a good forwarding candidate for its neighbors, improving the reliability of gradient routing.

Finally, the usage of *quantized* cost value itself is beneficial in gradient routing since it can enlarge the size of forwarding candidates set in gradient routing. Suppose a MANET scenario as shown in Fig. 3.7. Node D is the traffic destination and node A is the traffic source. Node A can communicate with node B and node C, but the link between node A and node C is unreliable due to long distance. Now, suppose that node D floods an UM and node C rebroadcasts the received UM after some random backoff time. Then, node A and node B succeed to receive the UM. If we use the cost as the traditional hop-count, node A and node B will set their cost toward node D as 2. Then, only node C is a possible forwarding candidate for node A since node B has the same cost with node A. This makes the packet forwarding be only available on the link between node A and node C, resulting in frequent retransmissions or packet drops. However, if we use the SNR-based link cost, the cost of node A is likely to be smaller than that of node B. This enables the packet to be delivered from node A to node C through node B if node C cannot receive the packet directly from node A. This results in the additional path diversity gain in gradient routing, improving the reliability of packet delivery.

3.4.3 Miscellaneous for efficient forwarding cancellation

In E-GRAD, a node with a transmission schedule always checks whether it is receiving a frame at the MAC layer when the backoff timer for the packet expires. If it is receiving a frame, it waits for the comple-

tion of the frame reception. Then, it transmits the scheduled packet if the received frame does not contain a data packet that satisfies the forwarding cancellation condition for the scheduled packet. This mechanism reduces the number of unnecessary packet transmissions in gradient routing.

Next, the backoff window size for data packet forwarding schedule is adjusted adaptively according to the length of the packet being scheduled. The objective is to keep the degree of wireless medium congestion at an acceptable level even though the packet length increases. In E-GRAD, nodes increase the backoff window size by twice if the length of the packet is larger than a threshold.

3.5 Simulation results

In this subsection, we evaluate the performance of E-GRAD through NS-3 based simulations.

3.5.1 System model

We consider a realistic MANET scenario where short-term fading effect and node mobility exist. We implemented a propagation loss model in NS-3 that considers both large-scale path loss (log-distance path loss [22]) and small-scale short-term fading effect (Nakagami- m fading [19]). Under this propagation loss model, the received signal strength, P_{RX} , at a receiver can be calculated according to the fol-

lowing equation.

$$P_{RX} = P_{TX} - PL_0 - \gamma \log_{10} \frac{d}{d_0} - X_{Fading}, \quad (3.5)$$

where P_{TX} is the signal transmission power in dBm, PL_0 is the loss at the reference distance d_0 , γ is the path loss exponent, d is the distance between the transmitter and the receiver, and X_{Fading} is the small-scale fluctuation component that follows Nakagami- m distribution.

We adopted the random way-point model [23] for emulating the mobility of nodes. In this mobility mode, every nodes are distributed randomly in a given two-dimensional space at the beginning of a simulation run. Then, every node randomly selects a point in a given two-dimensional space, and moves toward the point with randomly chosen speed within $[V_{MIN}, V_{MAX}]$. Whenever a node reaches to the point, it waits for a pause time, T_{PAUSE} , and picks up another point and moves toward it. This movement continues until the simulation finishes.

For the physical layer of wireless communication, we consider 802.11n-compliant model where orthogonal frequency division multiplexing (OFDM) modulation technique are used. The packet reception probability at a receiver is calculated according to the Nist error rate model [56], which takes the experienced signal-to-interference-plus-noise ratio (SINR) as the input argument. When a node w receives a frame that is transmitted by a node v , the SINR value is

calculated as follows.

$$SINR_w = \frac{P_{vw}}{N + \sum_{k \in V \setminus v} P_{kw}}, \quad (3.6)$$

where P_{vw} is the received power of node v 's transmission at node w that is obtained by the equation (3.5), N is the thermal noise floor, and P_{kw} is the interference experienced at node w due to the transmission of node k . Under this physical layer model, the packet reception probability is almost 1 before the distance between the receiver and the transmitter reaches to a certain threshold, then decreases sharply to 0 as the distance exceeds the threshold. Note that even though the distance is much smaller than the threshold, the packet reception probability is not 1 under Nakagami- m fading model since the received signal strength can become very low with some probability.

For the medium access control (MAC), we consider 802.11 distributed coordinate function (DCF) where binary exponential backoff based carrier sense multiple access / collision avoidance (CSMA/CA) is used. Note that the gradient routing assumes that the backoff function is implemented at the network layer, i.e., the MAC layer backoff is performed only if the network layer sends a data packet to the MAC layer after the expiration of the network layer backoff in the gradient routing.

3.5.2 Schemes in comparison

The schemes in comparison can be classified into three categories: oracle routing, gradient routing protocols, and hop-by-hop routing protocols.

Oracle routing

The operation of oracle routing is as follows. Suppose that a traffic source receives a packet from its upper layer at time t . Then, the source constructs a connectivity graph $G(V, E)$ using the position information of all nodes at time t . Here, V is the set of nodes and E is the set of edges. We consider that there exists an edge between a node v and a node w if the packet reception probability is larger than 0 after adopting the log-distance path loss only. The inverse of calculated packet reception probability becomes Expected Transmission Count (ETX) metric [52]. Then, the source finds a minimum cumulative ETX route using Dijkstra algorithm [24], and forward the packet to the next-hop node on the route via link-layer unicast. The next-hop node also constructs a connectivity graph, calculates a minimum cumulative ETX route, and forward the packet to the found next-hop. This procedure repeats until the packet reaches to the destination. We implement this oracle routing in order to figure out the performance on ideal routes.

Gradient routing protocols

We consider two different gradient routing approaches: E-GRAD and gradient routing with hop-count cost (GRAD (Hop)). E-GRAD differs from GRAD (Hop) in the type of the cost being used. In E-GRAD, when a node receives UM or URM, it sets its cost according to the algorithm 1 as described in subsection 2.4.2, while nodes using GRAD (Hop) always set their cost as the cost value in the UM or URM plus 1.

Hop-by-hop routing protocols

We consider four conventional hop-by-hop routing protocols which are designed for providing reliable unicast transmission in MANET: Ad-hoc on-demand distance vector (AODV) routing [4], destination-sequenced distance vector (DSDV) routing [8], optimized link-state routing (OLSR) [5], and dynamic source routing (DSR) [6]. In AODV and DSR, a traffic source discovers a route to the destination reactively, i.e., the routing protocols initiate the route discover process only if there is a traffic to serve. In DSDV and OLSR, every node broadcasts routing messages *periodically* which contains local or global topology information. This information is used for nodes to construct a routing table which consists of (destination, next-hop, cost) tuples in general. A traffic source in DSDV and OLSR can delivery a packet to the destination if it has a valid next-hop information toward the traffic destination.

3.5.3 Performance metrics

In order to evaluate the performance of schemes, we use four metrics: packet delivery ratio, per-session throughput, total number of transmissions for data delivery, and average end-to-end delay. The packet delivery ratio is the ratio of the number of received data packets to the number of generated packets for an end-to-end session. The per-session throughput is calculated as dividing the total number of received bits to the simulation time. The high value of per-session throughput is preferred. The total number of data transmissions represents the number of transmissions on the wireless channel that are performed to deliver data traffic. This metric represents the efficiency of schemes. Finally, the average end-to-end delay is the average time taken by each packet to be delivered from source to destination. For every scheme, we excluded the delay caused by the route discovery process in order to evaluate the efficiency of discovered route only.

3.5.4 Simulation environments

In the simulations, nodes are randomly distributed within a 500×500 m^2 area at the beginning of simulations. Then, they moves according to the random way-point model without pause time. Every node transmits data or routing packets with same rate (6 Mbps) and power (16.0206 dBm). The carrier sensing threshold that is -99 dBm and

the frame detection threshold is -96 dBm^2 . With this setting, the effective transmission range where the packet reception probability is larger than 0 is about 110 m.

In gradient routing protocols, we use two backoff window sizes in the forwarding procedure, 10 ms and 20 ms, according to the length of the packet. If the length of the packet is smaller than 512 bytes, we set the backoff window size of 10 ms. Otherwise, we set the backoff window size as 20 ms. The period of Update message broadcast is 10 seconds. With respect to the retransmission policy, hop-by-hop routing protocols (including oracle routing) directly adopt the link-layer retransmission mechanism. The maximum number of retransmissions at the link layer is 7. In gradient routing protocols, if a node that has transmitted a packet cannot overhear the transmission of same packet from lower-cost node within the backoff window, it can retransmit the packet maximum 2 times.

Finally, we ran 30 simulations for each case with different random seeds. The simulation results are averaged to get a bar or point in graphs, where error bars in the graphs represent the standard error.

3.5.5 Results

In this subsection, we analyze the simulation results in detail.

²If the received signal strength is between the carrier sensing threshold and the frame detection threshold, the receiver senses the channel is busy but cannot decode the frame. If the received signal strength is larger than the frame detection threshold, the transmitted frame can be decoded with a probability calculated by Nist error rate model.

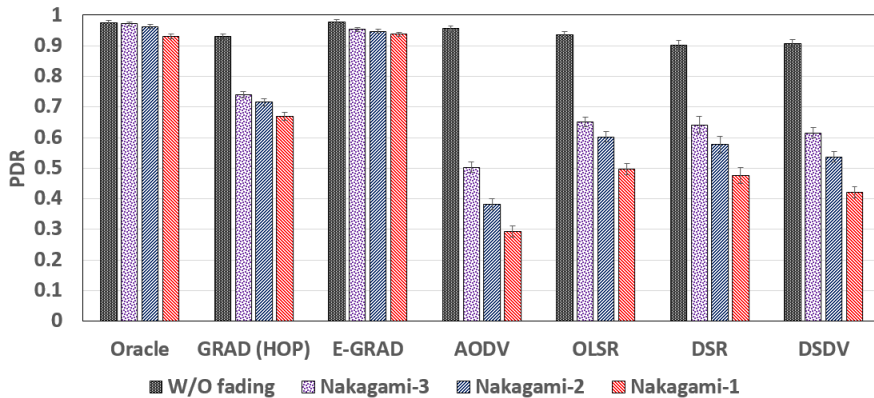


Figure 3.8: Packet delivery ratio under different fading coefficients.

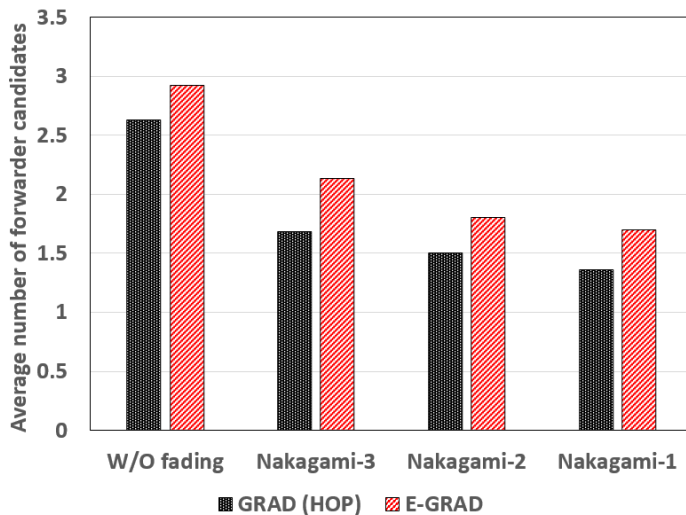


Figure 3.9: The average number of forwarder candidates for a node with forwarding schedule. In E-GRAD, more number of nodes participate in packet forwarding compared to GRAD (Hop).

Impact of short-term fading

Fig. 3.8 shows average PDR of each protocol under different fading coefficients. In this simulation, 10 end-to-end sessions are activated af-

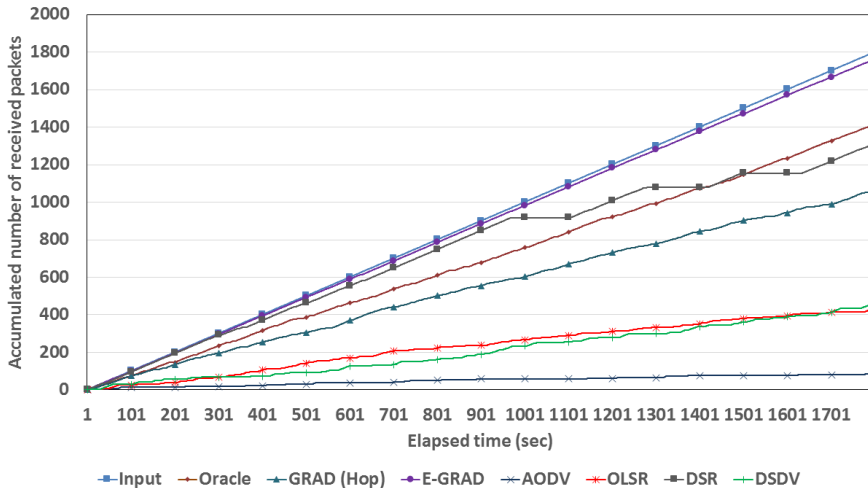
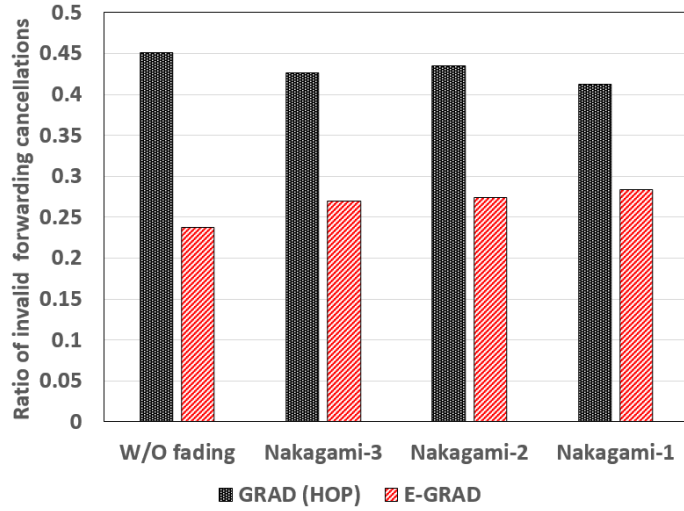


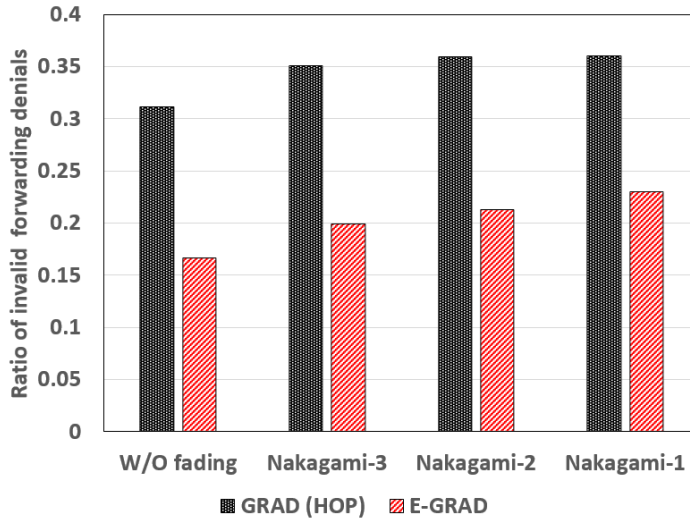
Figure 3.10: The accumulated number of delivered packets for a randomly-chosen end-to-end session as the simulation time elapses. We can see that E-GRAD delivers most of generated packets without bursty losses.

ter 60 seconds of warm up period, and generates traffic for 60 seconds with a constant rate of 1 packet per second. We fixed the position of nodes in order to figure out the impact of short-term fading only. First, we can see that E-GRAD achieves an ideal PDR similar to Oracle routing under all short-term fading models, thanks to its resilience on cost calculation errors and diversity effect.

We can figure out the reliability of routing protocols more clearly through tracing the accumulated number of delivered packets for a randomly-chosen end-to-end session as the simulation time elapses. Fig. 3.10 shows the result when we adopt Nakagami-1 fading model. Here, the steepness of a line represents the reliability of constructed forwarding mesh (in E-GRAD and GRAD (Hop)) or discovered lin-



(a) Ratio of invalid forwarding cancellation events



(b) Ratio of invalid forwarding denial events

Figure 3.11: The ratio of invalid operation events to all corresponding events. The ratio of invalid forwarding cancellations and denials is smaller in E-GRAD than in GRAD (Hop).

ear route (in Oracle and other conventional routing protocols), and the flat period represents the bursty packet losses incurred by route

discovery failures. As expected, E-GRAD delivers most of generated packets successfully without bursty losses. Oracle shows stable packet delivery trend, but it suffers from intermittent packet losses caused by MAC-layer retransmission failures³ With respect to conventional routing protocols, they experience from bursty packet losses even though the network topology is fixed. The reason is that routing protocols make wrong decision about the status of links when fading-oriented unexpected routing message losses occur, resulting in bursty packet losses during unnecessary route rediscovery procedures.

We can also confirm that SNR-based cost calculation improves the reliability of gradient routing through the PDR comparison with GRAD (Hop). First, using SNR-based cost increases the average number of neighboring nodes for a node that has smaller cost than the node as shown in Fig. 3.9. Second, using SNR-based cost improves the accuracy on forwarding decision and cancellation during gradient routing. Fig. 3.11a and Fig. 3.11b show the ratio of invalid forwarding cancellations and denials, respectively. If a node cancels its transmissions schedule after overhearing a transmission from a node whose distance to the destination is longer than itself, this forwarding cancellation is invalid. Similarly, if a node denies to forward a packet after receiving the packet from a node whose distance is longer than itself, this forwarding denial is invalid. We can see that the ratio of invalid operations in E-GRAD is smaller than that in GRAD (Hop).

³Note that ‘minimum-ETX’ does not equal to ‘minimum-loss-probability’.

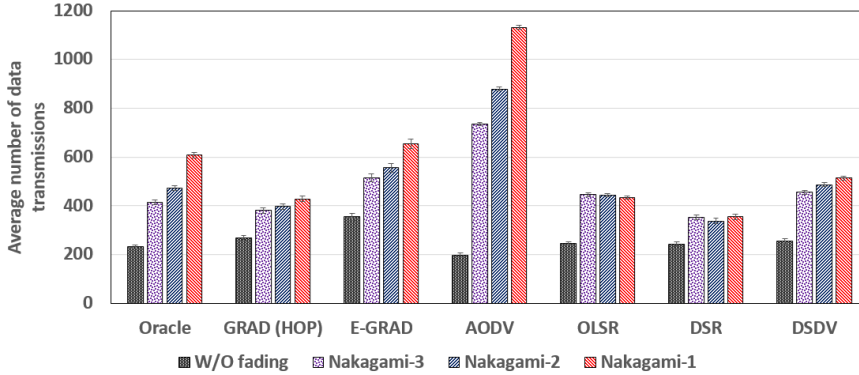


Figure 3.12: The number of transmissions used for data traffic delivery under different fading coefficients.

Conventional hop-by-hop routing protocols also show high PDR if there is no short-term fading effect. However, as the level of short-term fading increases, the PDR of conventional routing protocols decreases rapidly. There are mainly two reasons. First, the conventional routing protocols may fail to discover a route due to unexpected routing message losses during the route discovery process. Second, the routing protocols can include unreliable links on the found route due to errors in link quality estimation.

Of course, there is a cost for enhancing PDR performance in E-GRAD. Fig. 3.12 shows the number of transmissions used in data traffic delivery for every routing scheme. We can see that E-GRAD generates more number of transmissions than Oracle routing to achieve similar PDR performance at every fading model. Since E-GRAD exploits the diversity effect on packet forwarding to improve the reliability, there can be duplicate forwarding trials on the network. However,

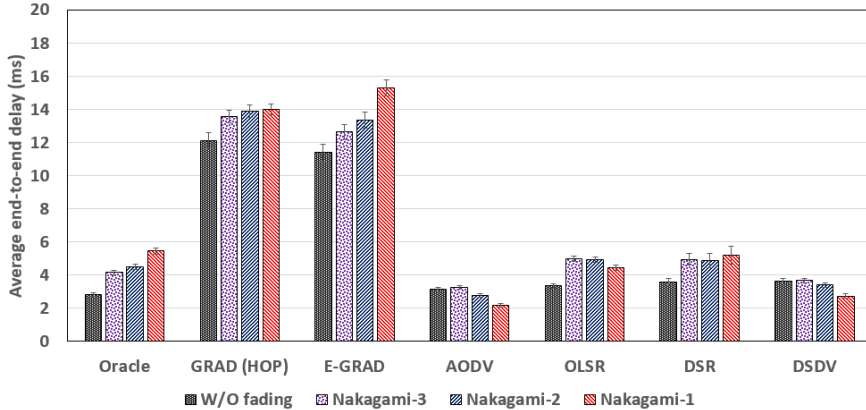


Figure 3.13: The average end-to-end delay of routing protocols under different fading coefficients.

the amount of increase was not so high in this simulation. AODV generates significant amount of transmissions due to temporal routing loops generated during the simulation, which is well-known problem in NS-2 based AODV implementations [25]. Other protocols show smaller communication cost than E-GRAD and Oracle routing, but they achieve much lower PDR than E-GRAD and Oracle.

Fig. 3.13 shows the average end-to-end delay performance of routing protocols. First, in Oracle routing, the delay increases as the short-term fading effect becomes severer due to frequent retransmissions in MAC layer. E-GRAD experiences higher end-to-end delay than Oracle routing mainly for two reasons. First, E-GRAD accompanies large-scale network-layer backoff at each forwarding step. Second, data packets in E-GRAD can be delivered to their destination through non-minimum-ETX route due to the path diversity.

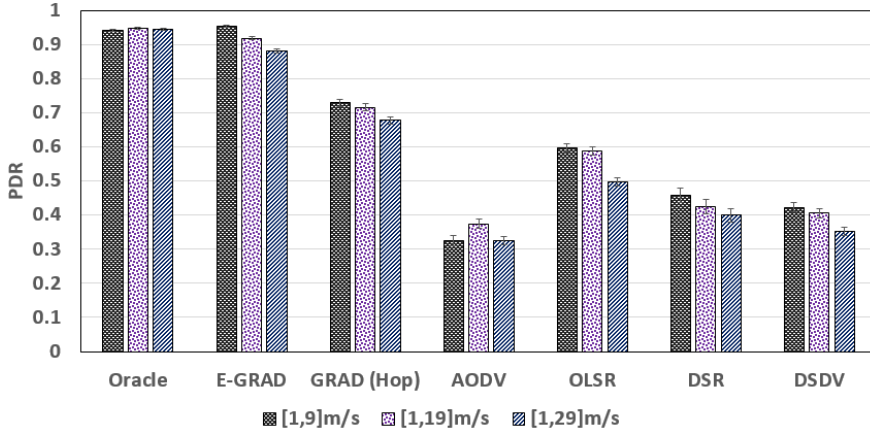


Figure 3.14: The packet deliver of routing protocols under different node mobility.

General performance under mobility

Fig. 3.14 shows the packet delivery ratio of routing protocols under different node mobility, i.e., different values for $[V_{MIN}, V_{MAX}]$. In this simulation, Nakagami-1 (Rayleigh) fading model is used. According to Fig. 3.14, we can see that the packet delivery ratio of practical routing protocols decreases as the mobility of nodes increases even though there are possible communication route as Oracle routing reveals.

The main reason is due to the expiration of cost or route information obtained from control message exchanges. In conventional hop-by-hop routing protocols, the data packet can be dropped if the current route includes some links that has been already broken. There are several mechanisms for overcoming the link breakages in conventional hop-by-hop routing protocols, but they are insufficient to provide an ideal packet delivery ratio as Oracle routing. E-GRAD also

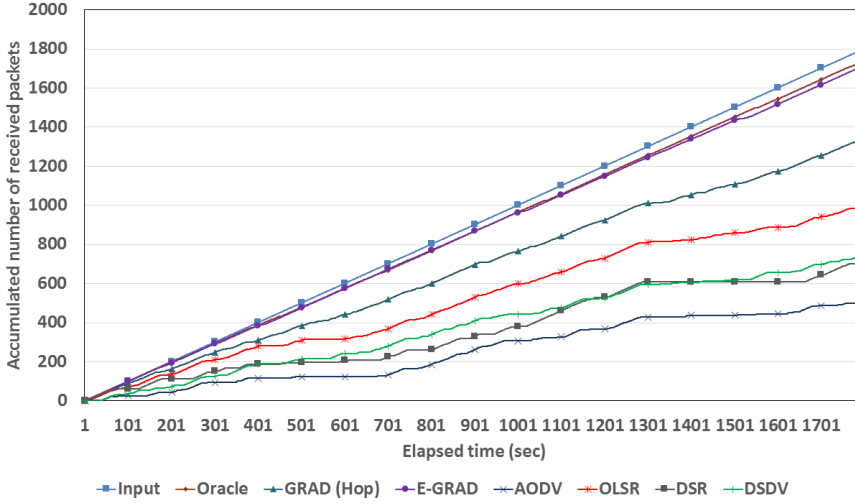


Figure 3.15: The accumulated number of delivered packets for a randomly-chosen end-to-end session as the simulation time elapses. Here, the speed of nodes are chosen within $[1,9]$ m/s. We can confirm that E-GRAD provides reliable unicast service even though there are errors in the estimated cost.

experience same problem of cost information expiration, but the performance degradation is not so severe thanks to its resilience on cost calculation errors. The packet delivery tracing results in Fig. 3.15 also supports the above explanation.

Fig. 3.16 shows the number of transmissions used in data traffic delivery under different node mobility. First, we can see that E-GRAD consumes more transmission times than Oracle routing due to its diversified forwarding. Second, we can see that conventional hop-by-hop routing protocols consume comparable transmission times like Oracle routing and E-GRAD even though their packet deliver ratio is lower than Oracle routing and E-GRAD. This means that numerous num-

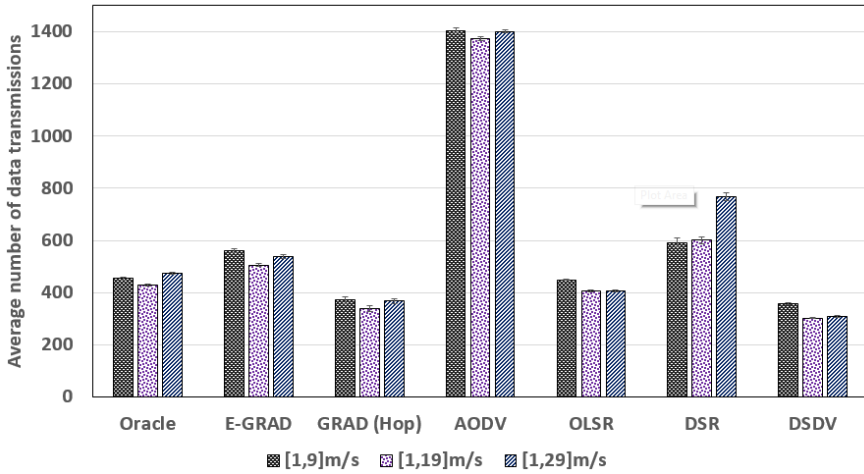


Figure 3.16: The number of transmissions used for data traffic delivery under different node mobility.

ber of transmissions end in vain at intermediate nodes which maintain invalid (i.e., already disconnected) next-hop information. The high value in AODV is due to temporal routing loops generated during the simulation.

Fig. 3.17 shows the average end-to-end delay performance of routing protocols. We can see that there is no notable relationship between the delay performance and node mobility. Actually, under low traffic load, the end-to-end delay is dominated by the length of the forwarding path that a packet travels. In this simulation, the position of nodes are restricted on an area with fixed size, thus the mobility of nodes does not influence the length of the forwarding path significantly.

The conventional hop-by-hop routing protocols except for AODV show small end-to-end delay because of their packet delivery failure

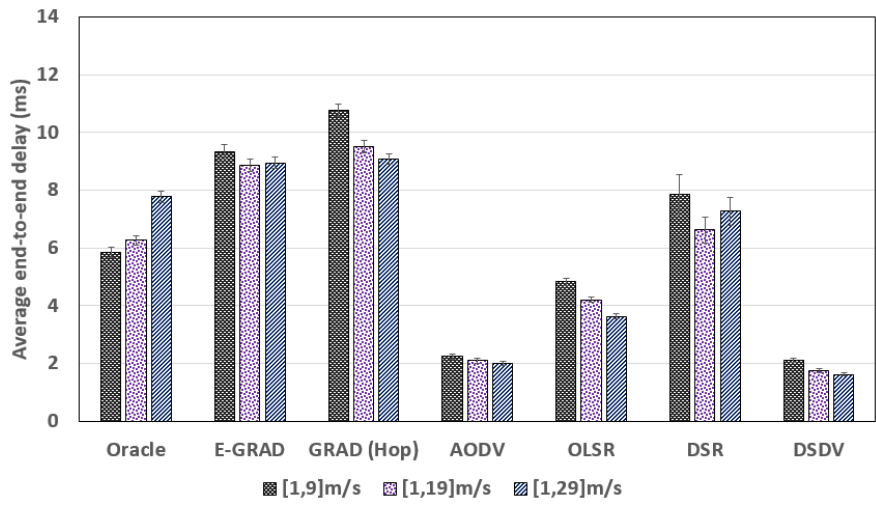


Figure 3.17: The average end-to-end delay of routing protocols under different node mobility.

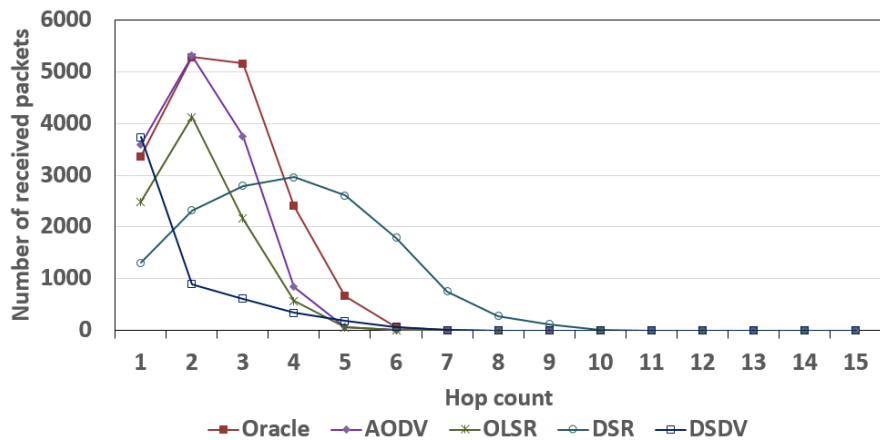


Figure 3.18: The number of received packets according to the traveled hop count.

for distant end-to-end sessions. As shown in Fig. 3.18, the number of received packets in OLSR, DSDV, and AODV drops rapidly as the traveled hop-count increases unlike Oracle routing. E-GRAD shows

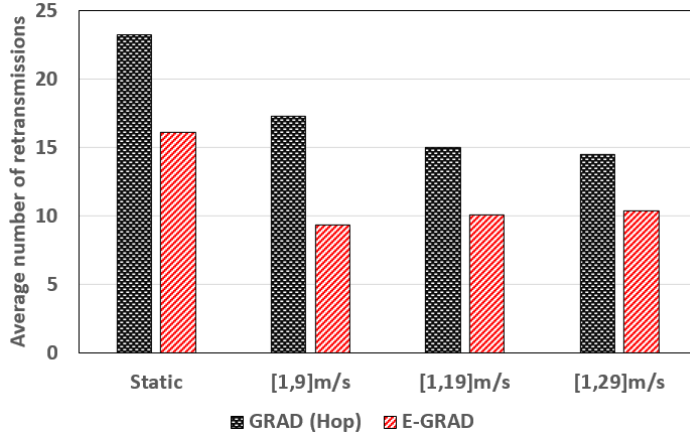


Figure 3.19: The average number of network-layer retransmissions in the procedure of gradient routing. GRAD (Hop) yields more number of retransmissions than E-GRAD.

similar delay performance with GRAD (Hop) even though the packet delivery ratio is higher than it. The reason is that packets experiences more number of network-layer retransmissions in GRAD (Hop) than in E-GRAD as shown in Fig. 3.19.

With different offered load

Fig. 3.20 and Fig. 3.21 represent the average per-session throughput and average end-to-end delay with different offered load, respectively. In this simulation, 5 end-to-end sessions are activated after 60 seconds of warm up period, and generates traffic for 60 seconds with a constant rate from 20 kbps to 160 kbps. The data packet size is 1024 bytes. We fixed the position of nodes and considered Nakagami-1 fading.

We can see that E-GRAD achieves comparable throughput with

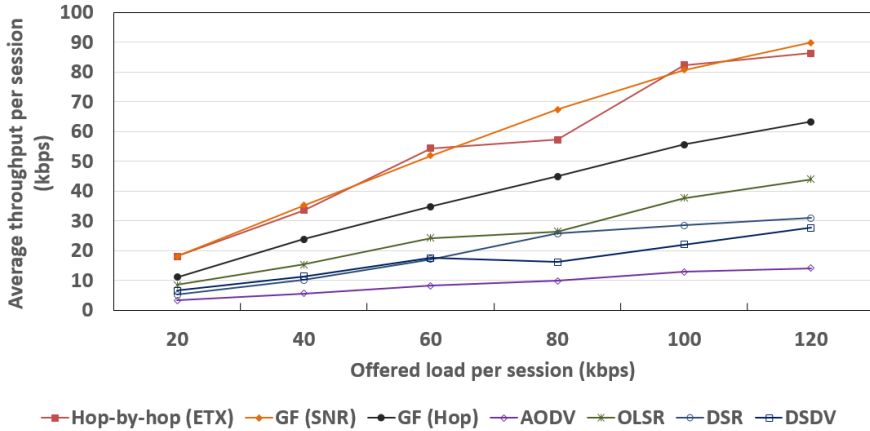


Figure 3.20: The average per-session throughput with different offered load.

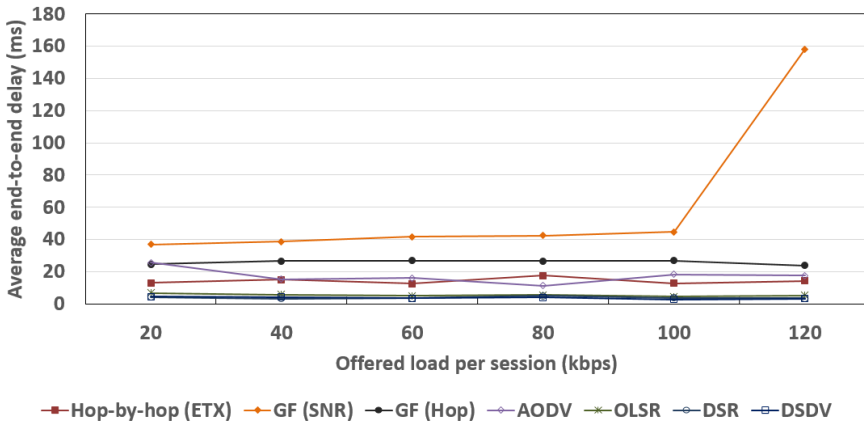


Figure 3.21: The average end-to-end delay with different offered load.

Oracle routing incurring stable end-to-end delay performance until the offered load reaches to the network capacity bound, in this simulation, about 100 kbps for each session. This means that the forwarding cancellation mechanism in gradient forwarding successfully manages the level of congestion in wireless channel under acceptable traffic

load. Of course, the average end-to-end delay increases rapidly in E-GRAD after the wireless channel becomes saturated.

3.6 Related work

Our research is motivated from the original version of gradient routing design [12]. It also considers an on-demand cost update procedure which is similar to that in E-GRAD, but there are some differences. In E-GRAD, UM receivers rebroadcast it if TTL value in the UM is larger than 1. However, in the original version, the destination of a traffic specifies the source (i.e., the origin of URM) when it broadcasts an UM. Then, nodes that has smaller cost to the source participates in the flooding of UM. This destination-specific UM broadcast can reduce the communication overhead for cost update. However, it also limits the number of forwarder candidates.

In addition, the original version takes a reactive approach for UM generation: if the source experiences several packet drops, it re-initiate cost update procedure by broadcasting new URM. This approach is not suitable for traffic that requires seamless unicast service. The authors also suggest the use of SNR-based cost for gradient routing in their patent application [13]. However, the cost calculation function is different from ours, and they do not provide any analysis or simulation results that can reveal the advantage of SNR-based cost on gradient routing. To the best of our knowledge, this is the first work

that elaborates the gradient routing protocol with on-demand cost update and SNR-based cost calculation, which shows superior performance over conventional hop-by-hop routing protocols under realistic MANET scenarios.

3.7 Summary

In this chapter, we investigate two well-known unicast service mechanisms in MANET (hop-by-hop routing and gradient routing) and verify the superiority of gradient routing over hop-by-hop routing in terms of reliability in unicast transmission. Based on the understanding, we propose a practical gradient forwarding architecture (E-GRAD) using on-demand cost update scheme with SNR-based cost calculation. Simulation results show that E-GRAD can achieve an ideal packet delivery ratio (or throughput) performance under low and moderate traffic load with acceptable level of communication overhead.

Chapter 4

Access-GRAD: A Gradient Routing Protocol for Uplink and Downlink Unicast in Wireless Multi-hop Access Networks

4.1 Introduction

In Chapter 3, we confirm that E-GRAD provides reliable unicast service in realistic MANET scenarios. Motivated by this result, we pro-

pose a modified version of E-GRAD that is optimized for wireless multi-hop access networks. Unlike general MANETs, wireless multi-hop access network has a hierarchical network architecture. They consist of a gateway node and multiple mobile devices. The gateway node is connected to the internet, and provides communication service to the mobile devices through direct or multi-hop relaying. In this situation, the traffic direction can be either from the gateway to a mobile device (downlink), or from a mobile device to the gateway (uplink).

The main idea of the proposed scheme is to build a cost field toward the gateway node by relaying a tone-signal from the gateway node to mobile devices on different subcarriers, and use the cost for both uplink and downlink gradient routing. In uplink gradient routing, the cost is used for forwarding decision and cancellation directly. In downlink gradient routing, the cost is used in conjunction with uplink transmission history at mobile stations. By doing so, we can provide reliable uplink and downlink unicast in wireless multi-hop access networks with very small cost management overhead.

The rest of this chapter is organized as follows. In Section 2, we briefly explain the system model. In Section 3, we explain our proposed scheme in detail. Simulation results are presented in Section 4. Finally, we summarize this chapter in Section 5.

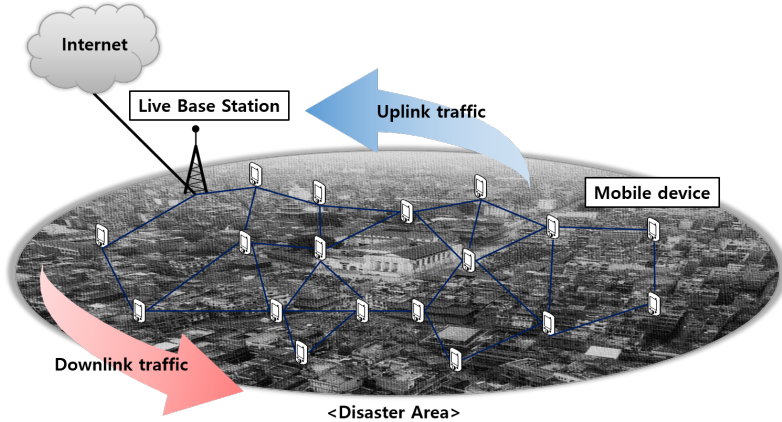


Figure 4.1: A smart-phone based disaster recovery network. A live base station and mobile devices can communicate with each other multi-hop wireless links.

4.2 System model

We consider a wireless multi-hop access network where every node equips with an Orthogonal Frequency Division Multiplexing (OFDM) based radio transceiver. The total number of data subcarriers is N_S , and we assume that a tone-signal can be transmitted and detected on per-subcarrier basis [42, 43]. In addition, we assume that the maximum hop-distance between the gateway and a station node is smaller than N_S .

Smart-phone based disaster recovery network [27] can be a good example of wireless multi-hop access networks which uses OFDM as the physical layer technology. In a disaster situation, such as earthquake or hurricane, the communication service in the disaster area may be restricted since the communication infrastructure can be dam-

aged. However, if there is live cellular base stations or wireless LAN access points, smart-phone users in the area can connect to the internet by constructing a wireless multi-hop access network that consists of a live gateway and themselves. Fig. 4.1 describes an example case.

For the wireless channel access, we assume that every node operates carrier sense multiple access / collision avoidance (CSMA/CA) mechanism [60]. Under CSMA/CA, a node senses the wireless channel before transmitting a frame. If the node detects the channel idle for a predefined time of long inter-frame space, *LIFS*, then it transmits the frame immediately. Otherwise, it attempts to transmit it again after some random backoff time.

4.3 Access-GRAD

In this section, we introduce our proposed scheme in detail.

4.3.1 Tone-signal based cost update

In the proposed scheme, the gateway node periodically transmits a tone-signal on the *first* subcarrier among N_S subcarriers for a short duration, T_{TONE} . Nodes that detect this tone-signal check whether their *ToneRxFlag* is 0. If so, they update their cost toward the gateway node based on the subcarrier index where a tone-signal has been detected, and the measured SNR during the reception of the tone-signal. We explain the cost calculation algorithm later. Then, they

set $ToneRxFlag$ as 1. This $ToneRxFlag$ becomes 0 after a predefined time, $T_{REFRESH}$. With $ToneRxFlag$ as 1, any detection of a tone-signal is ignored. After that, they transmit a tone-signal on the *second* subcarrier among N_S subcarriers after a short inter-frame space, $SIFS$, from the tone-signal reception. Like this, if a node detects a tone-signal on i 'th subcarrier, it update its cost toward the gateway, set $ToneRxFlag$ as 1, and transmit a tone-signal on $(i + 1)$ 'th subcarrier.

Now, we explain the cost calculation algorithm. Suppose that node A detects a tone-signal on i 'th subcarrier. Then, if the measured SNR of the tone-signal, SNR_{TONE} , is larger than SNR_{THRES} , node A sets its cost toward the gateway node, C_A , according to the following equation.

$$C_A = (i - 1) \times SNR_{THRES}. \quad (4.1)$$

Otherwise, C_A is set as follows.

$$C_A = (i - 1) \times SNR_{THRES} + \lceil SNR_{THRES} - SNR_{TONE} \rceil. \quad (4.2)$$

The first part of Equ. (4.1) and Equ. (4.2) is an offset cost that reflects the topological distance between the gateway and node A . Since the subcarrier index increases monotonically when a node relays a tone-signal, node A can regard the subcarrier index i as the number of hop count from the gateway node. Therefore, the subcarrier index i contributes to the offset cost of C_A . The second part of Equ. (4.1) and

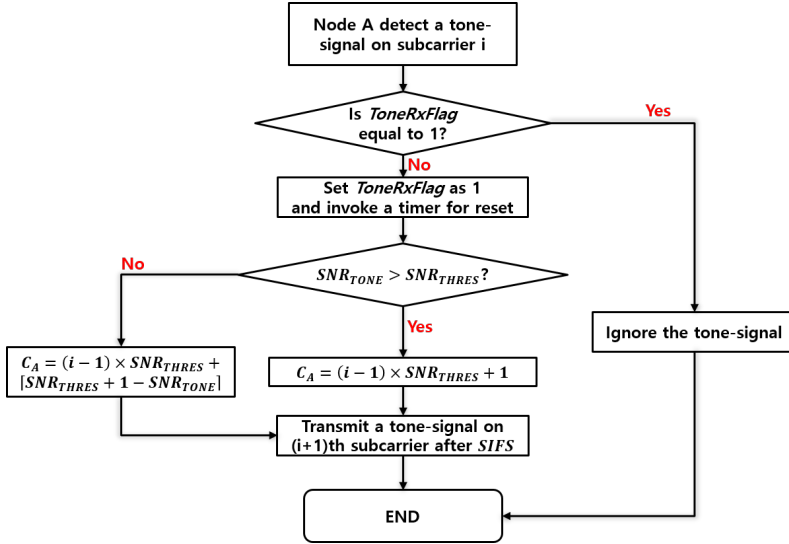


Figure 4.2: The operation flow diagram of node A when it detects a tone-signal on subcarrier i .

Equ. 4.2 is a cost that reflects the quality of link between node A and tone-signal transmitters. If node A detects a tone-signal with high SNR, node A decides that it has reliable forwarding candidates for uplink unicast, and just adds 1 to C_A . Otherwise, node A intentionally increases C_A as shown in Equ. (4.2). Fig. 4.2 describes the operation flow of a node that detects a tone-signal on subcarrier i .

The main advantage of tone-signal based cost update is the reduction of communication overhead. In E-GRAD, the cost update is accomplished by flooding a network-layer control message (Update message) with backoff mechanism, which takes long time to disseminate Update messages. However, in the proposed tone-signal based cost update, multiple nodes *concurrently* transmit a tone-signal on

subcarrier $(i + 1)$ just after a *SIFS* of the tone-signal detection on subcarrier i without backoff. Therefore, every tone-signal relaying occupies the wireless medium for $T_{TONE} + SIFS$ which can be a very short time, resulting in the rapid completion of cost update procedure.

Additionally, we can improve the reliability of tone-signal update by restricting the transmissions of mobile devices while cost update procedure is ongoing. Suppose that a node detects a tone-signal on subcarrier i at time t . Then, if it knows the tone-signal generation period at the gateway, T_{TG} , then it can infer the beginning of the next tone-signal dissemination, $t(next)$, as follows.

$$t(next) = t + T_{TG} - i \times (T_{TONE} + SIFS). \quad (4.3)$$

Therefore, if we suppress the transmissions of mobile devices from $t(next)$ to $t(next) + N_S \times (T_{TONE} + SIFS)$, the cost update procedure can be completed without any interruption from data transmissions.

4.3.2 History based gradient routing for downlink transmission

After tone-signal based cost field construction, the uplink traffic can be served through gradient routing. However, serving downlink traffic through gradient routing is not straightforward. Intuitively, we can adopt E-GRAD to serve the downlink traffic. However, E-GRAD requires per-destination cost management that relies on Update mes-

sage flooding. Therefore, the wireless channel can be congested due to numerous Update message transmissions if downlink data packets are destined to a number of different mobile stations.

In order to suppress the communication overhead for cost management, we propose a new downlink gradient routing scheme. The key idea is to confine the forwarding participants in downlink gradient routing to nodes that have the history of uplink packet reception. In the proposal, if a node receives an uplink data packet, it caches the source of the packet in its *uplink history table (UHT)*. The cached information is removed if the node cannot receive any uplink packet originated from the cached node within T_{VALID} .

Now, suppose that the gateway node has a downlink packet toward node A . Then, it first checks whether it has node A in its *UHT*. If so, it transmits the packet that includes the cost toward the gateway (in this case, '0'). Also, it sets *GRFlag* in the header as '1' in this case. Then, nodes that receive a downlink packet with *GRFlag* '1' also checks their *UHT*, and decides to forward the packet if they find the destination in their *UHT* and their cost toward the gateway is larger than the value in the packet. Finally, the scheduled forwarding is canceled if the node with a schedule overhears a packet that contains *larger* cost toward the gateway node.

If the gateway node fails to find the destination of downlink traffic in its *UHT*, it sets *GRFlag* field in the packet header as '0', and just floods the packet since the gradient routing is impossible due to the

Algorithm 2 The operation of the gateway node

Notations

$UHT_{GATEWAY}$: The uplink history table of the gateway
 C^P : The cost value included in the packet P

Algorithm

- 1: The gateway node has a downlink packet P destined to node A .
 - 2: **if** $A \in UHD_{GATEWAY}$ **then**
 - 3: Transmit the packet with $GRFlag = 1$ and $C^P = 0$
 - 4: **else**
 - 5: Transmit the packet with $GRFlag = 0$ and $C^P = 0$
 - 6: **end if**
-

absence of uplink reception history. Then, any node that receives a downlink data packet with $GRFlag$ '0' retransmits it after random backoff time. Algorithm 2 and Algorithm 3 summarizes the operation of the gateway node and mobile devices for downlink transmission, respectively.

Additionally, if the gateway has many downlink packets toward a destination, it can invoke an uplink packet transmission from the downlink packet destination in order to serve the packets through proposed downlink gradient routing.

4.4 Performance evaluation

In this section, we present the simulation results. We implemented the proposed scheme in NS-3 simulator. The structure of the simulator is shown in Fig. 4.3. For the network layer, we implemented a routing module that performs gradient routing. In MAC layer, a tone-signal

Algorithm 3 The operation of non-gateway nodes

Notations

- UHT_v : The uplink history table of node v
 C^P : The cost value included in the packet P
 C_v : The cost value of node v toward the gateway

Algorithm

- 1: Node B receives a downlink packet P destined to node A .
 - 2: **if** P is duplicate **then**
 - 3: **if** $GRFlag == 0$ **then**
 - 4: Ignore P
 - 5: **else if** $GRFlag == 1$ **then**
 - 6: **if** $C^P > C_B$ **then**
 - 7: Cancel the forwarding schedule for P if exist
 - 8: **end if**
 - 9: **end if**
 - 10: **else**
 - 11: **if** $GRFlag == 0$ **then**
 - 12: Transmit P after random backoff time
 - 13: **else if** $GRFlag == 1$ **then**
 - 14: **if** $A \in UHT_B$ **then**
 - 15: Set C^P as C_B
 - 16: Schedule the transmission of P after random backoff
 - 17: **else**
 - 18: Ignore P
 - 19: **end if**
 - 20: **end if**
 - 21: **end if**
-

manager notifies the subcarrier and SNR information when it detects a tone-signal. Then, the routing module calculates the cost toward the gateway node based on the obtained information.

We compared the performance of Access-GRAD with Oracle routing described in Chapter 3.5.2, E-GRAD, and four conventional hop-by-hop routing protocols, AODV [4], DSDV [8], DSR [6], and OLSR [5],

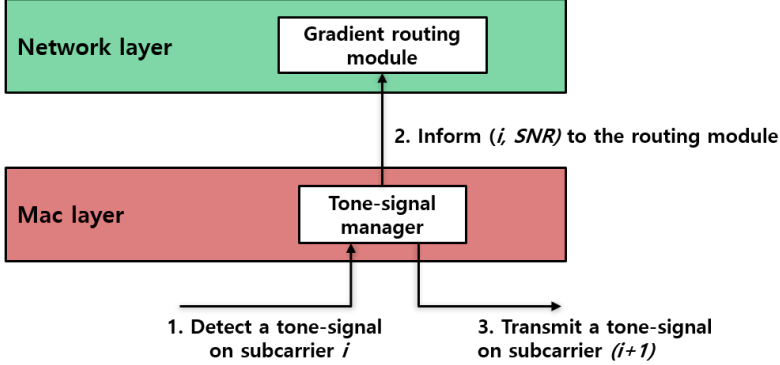


Figure 4.3: The structure of the simulator. We implemented a gradient routing module in the network layer, and a tone-signal manager block in the MAC layer.

Table 4.1: System parameters of the proposed scheme

Parameter	Value
SNR threshold for cost calculation (SNR_{THRES})	10 dB
Transmission time of a tone-signal (T_{TONE})	16 <i>usec</i>
Short inter-frame spacing (<i>SIFS</i>)	9 <i>usec</i>
Long inter-frame spacing (<i>LIFS</i>)	34 <i>usec</i>
Refresh timeout for $RxToneFlag$ ($T_{REFRESH}$)	1 sec
Tone-signal generation period (T_{TG})	10 sec
Number of data subcarriers (N_S)	48

which are developed for reliable unicast in wireless mobile ad-hoc networks. We use all parameters in conventional routing protocols as default values defined in NS-3. In E-GRAD, the gateway node floods Update message with a period of 10 seconds. In the proposed scheme, the gateway node transmits a tone-signal on the first subcarrier with a period of 10 seconds. Other system parameters of the proposed scheme is summarized in Table 4.1.

We consider that every node equips with 802.11n-compatible MAC / PHY transceiver in the simulation. Every node transmits with same transmission power (16.0206 dBm) for both tone-signal and data frame. The data transmission rate is 6 Mbps. We adopt a practical propagation loss model that considers distance-driven path loss and Rayleigh fading effect. Under this setting, the transmission range is about 100 m.

We consider wireless multi-hop access networks with 1 gateway node and 50 mobile devices. Every node is distributed on a square area with $500 \times 500 \text{ m}^2$ size. The position of the gateway node is fixed at (50, 50), while mobile devices move around the gateway node according to the random way-point mobility model [23]. In every simulation run, we activate 10 uplink sessions and 10 downlink sessions after 60 seconds of warm-up period. Each session generates data traffic with a rate of 1 packet/second, and continues for 60 seconds. Finally, all simulations are repeated on 30 randomly-generated topologies

4.4.1 Uplink performance

Fig. 4.4 shows the average packet delivery ratio of uplink sessions with different node mobility. We can see that Access-GRAD achieves a comparable packet delivery ratio with Oracle routing in every mobility scenario. E-GRAD shows a similar performance with Access-GRAD until the maximum node speed is 15 m/s. After that, Access-GRAD outperforms E-GRAD. Since the tone-signal based cost update com-

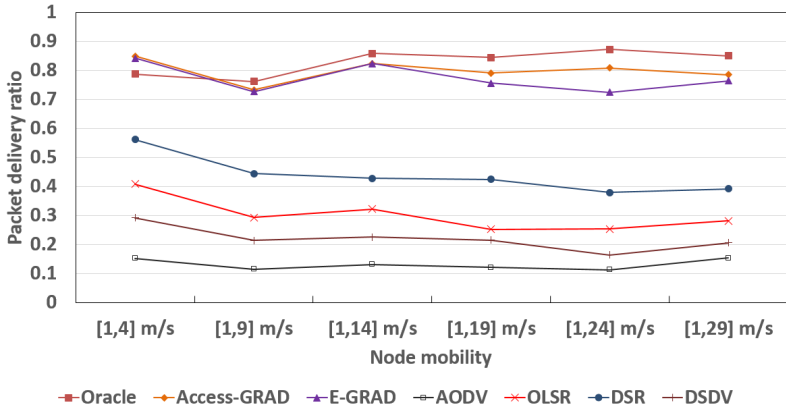


Figure 4.4: The average packet delivery ratio of uplink sessions with different node mobility.

pletes much earlier in Access-GRAD than in E-GRAD (0.42 msec vs 561.23 msec on average), nodes in Access-GRAD can maintain time-accurate cost values under high mobility, resulting in the increment of packet delivery ratio over E-GRAD. Meanwhile, conventional hop-by-hop routing protocols show very poor performance since they cannot react to the topology change properly. However, DSR performs better than AODV, DSR, and DSDV in this simulation. Actually, DSR also provides a level of path diversity since the source node in DSR can cache multiple routes to the destination that are discovered from the route discovery procedure, use them sequentially in the case of link failures [6].

Fig. 4.5 shows the average number of transmissions for uplink sessions with different node mobility. In this graph, we can confirm the reason of high packet delivery ratio in Access-GRAD: it consumes

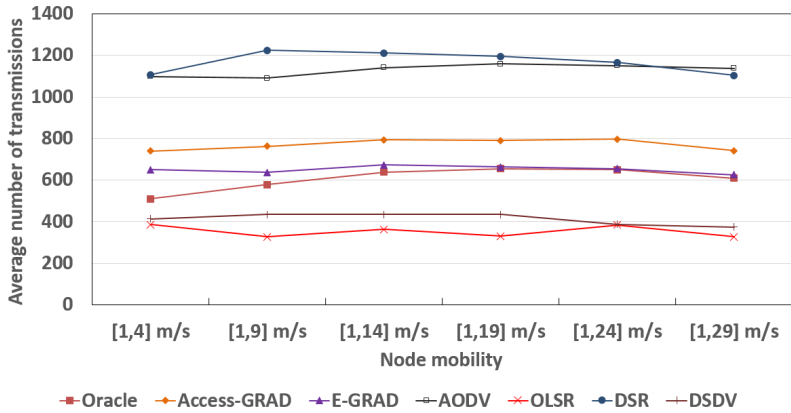


Figure 4.5: The average number of transmissions for uplink sessions with different node mobility.

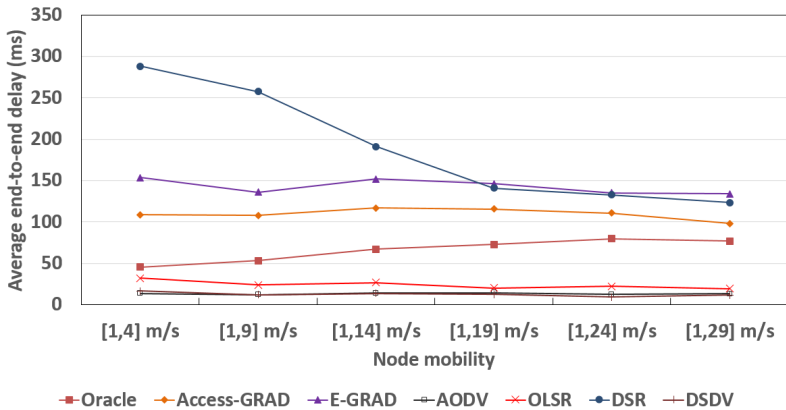


Figure 4.6: The average end-to-end delay of uplink traffic with different node mobility.

more communication resources for providing diversity gain. Conventional hop-by-hop routing protocols also consume comparable amount of wireless resources, but they fail to serve uplink traffic.

Fig. 4.6 shows the average end-to-end delay of uplink traffic with different node mobility. First, we can see that Access-GRAD delivers

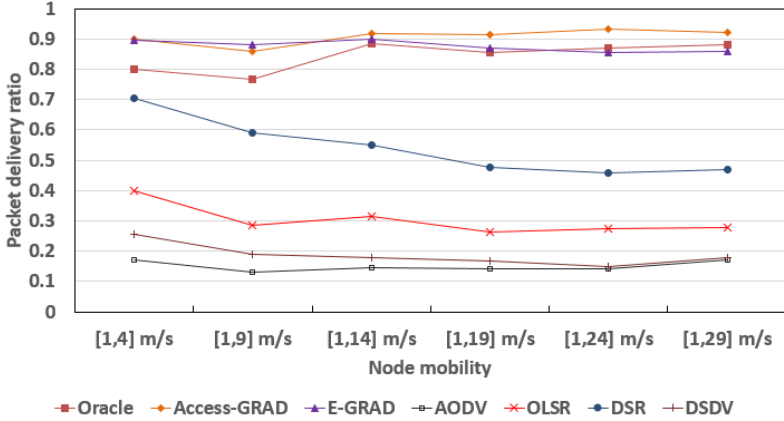


Figure 4.7: The average packet delivery ratio of downlink sessions with different node mobility.

the uplink packet more earlier than E-GRAD thanks to the time-accurate cost field generation. AODV, OLSR, and DSDV show very small delay since most of them fail to deliver data packets originated from distant mobile nodes. However, DSR experiences large end-to-end delay under node mobility [1,14] m/s thanks to its more success on packet delivery.

4.4.2 Downlink performance

Fig. 4.7 shows the average packet delivery ratio of downlink sessions with different node mobility. Interestingly, Access-GRAD shows even better performance than Oracle routing in all mobility scenarios. The reason is that the set of forwarding candidates becomes larger in the proposed history based downlink gradient routing. As shown in Fig. 4.8, we can see that Access-GRAD consumes relatively larger amount

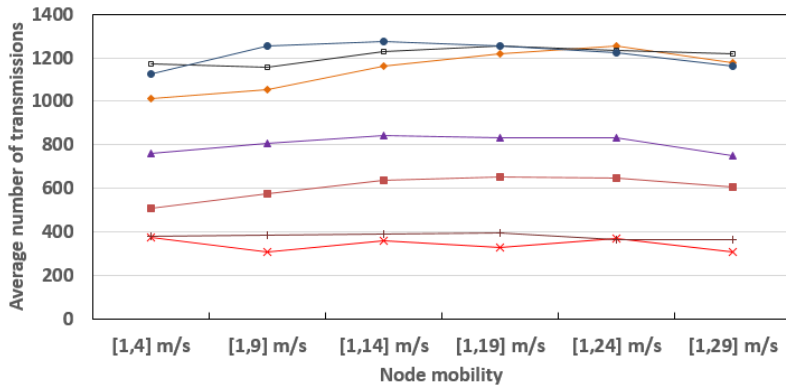


Figure 4.8: The average number of transmissions for downlink sessions with different node mobility.

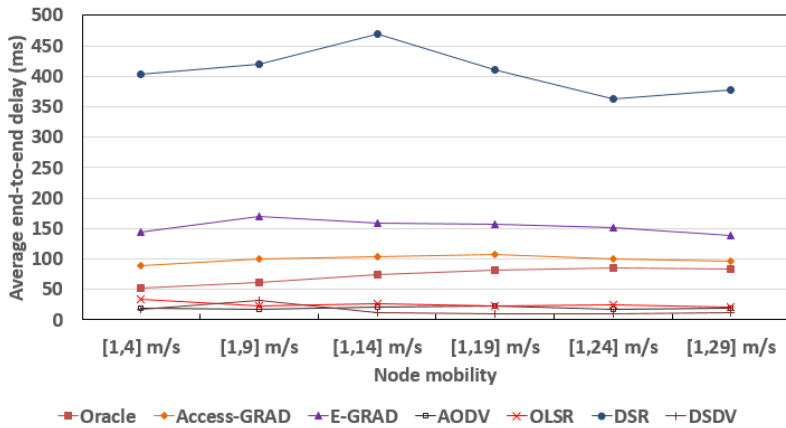


Figure 4.9: The average end-to-end delay of downlink traffic with different node mobility.

of wireless resources in downlink case even though the offered traffic is same for both uplink and downlink.

Fig. 4.9 shows the average end-to-end delay of downlink sessions with different node mobility. The trend is similar to the uplink case. DSR shows high delay performance due to its repetitive delivery trials

using cached routes. Access-GRAD shows higher delay than Oracle routing due to network-layer backoff and longer-path delivery, but provides lower delay than E-GRAD. AODV, OLSR, and DSDV also show low delay due to frequent packet delivery failures.

4.5 Summary

In this chapter, we proposed a modified version of E-GRAD (Access-GRAD) that is optimized for a special case of MANET: wireless multi-hop access networks. Unlike E-GRAD, nodes in Access-GRAD do not construct a cost field toward every destination, but they only construct a cost field toward a unique gateway node by relaying a tone-signal sequentially on data subcarriers. The constructed cost field is used for both uplink and downlink gradient routing. Specifically, the uplink transmission history of non-gateway nodes is used for confining the set of forwarding participants in downlink gradient routing. Through NS-3 based simulations, we confirmed that the proposed scheme enables reliable uplink and downlink unicast.

Chapter 5

Conclusion

5.1 Research contributions

In this dissertation, we proposed the routing schemes for efficient broadcast/unicast communication services in MANET.

First, we proposed a scalable broadcast protocol that achieves high packet delivery ratio with small communication overhead. In ST-BCAST, a node schedules the transmission of a broadcast packet only if it detects an explicit request for the packet from its neighbors. The packet transmission is delayed for a random backoff time and can be canceled in the meantime if the transmitter is notified of the packet reception from its neighbor(s). A false forwarding cancellation can be recovered by repetitive requests from the neighbors. We verified the reliability of ST-BCAST by showing that it satisfies two sufficient conditions for the complete delivery of a broadcast packet. In addition,

we confirmed the feasibility of subcarrier-level tone-signaling through simple experiments using USRP devices. Finally, we showed that ST-BCAST outperforms existing broadcast schemes with respect to the reliability and efficiency through NS-3 simulation.

Second, we investigated two well-known unicast service mechanisms in MANET (hop-by-hop routing and gradient routing) and verified the superiority of gradient routing over hop-by-hop routing in terms of reliability in unicast transmission. Based on the understanding, we proposed a practical gradient forwarding architecture (E-GRAD) that uses on-demand cost update scheme with SNR-based cost calculation. Through extensive simulations, we showed that E-GRAD achieves an ideal packet delivery ratio (or throughput) that can be achieved through minimum accumulated ETX route with moderate increase in communication overhead.

Lastly, we proposed a modified version of E-GRAD (Access-GRAD) that is optimized for a special case of MANET: wireless multi-hop access networks. Unlike E-GRAD, nodes in Access-GRAD does not construct a cost field toward every destination, but they only construct a cost field toward a unique gateway node by relaying a tone-signal sequentially on data subcarriers. The constructed cost field is used for both uplink gradient routing and downlink gradient routing. Specifically, the uplink transmission history of non-gateway nodes is used for confining the set of forwarding participants in downlink gradient routing. Through NS-3 based simulations, we confirmed that

the proposed scheme enables reliable uplink and downlink unicast.

5.2 Future research directions

There are several open problems in this dissertation.

- The design of ST-BCAST and Access-GRAD highly rely on the tone-signal transmission and detection capability. In this dissertation, we just verified the feasibility of tone-signal based signaling through simple experiments using USRP devices. We leave the implementation of ST-BCAST and Access-GRAD on the common-off-the-shelf devices as future work.
- In Access-GRAD, if mobile devices can be synchronized in time by estimating the elapsed time from the tone-signal generation, each node can access the wireless channel in a scheduled manner. We leave the design of an efficient medium access protocol in synchronized wireless multi-hop access networks as future work.

Bibliography

- [1] J. L. Burbank, P. F. Chimento, B. K. Haberman, and W. T. Casch, “Key Challenges of Military Tactical Networking and the Elusive Promise of MANET Technology,” *IEEE Commun. Mag.*, vol. 44, no. 11, pp. 39–34, Nov. 2006.
- [2] F. Li and Y. Wang, “Routing in Vehicular Ad hoc Networks: A Survey,” *IEEE Vehicular Tech. Mag.*, vol. 2, no. 2, pp. 12–22, Jun. 2007.
- [3] A. Howard, M. J. Matarić, and G. S. Sukhatme, “Mobile Sensor Network Deployment using Potential Fields: A Distributed, Scalable Solution to the Area Coverage Problem,” *Distributed Autonomous Robotics systems*, vol. 5, pp. 299–308, 2002.
- [4] C. E. Perkins and E. M. Royer, “Ad-hoc On-demand Distance Vector Routing,” in *Proc. IEEE Workshop on Mobile Computing Systems and Applications (WMCSA '99)*, 1999, pp. 90–100.

- [5] T. Clausen and P. Jacquet, “Optimized Link State Routing Protocol (OLSR),” RFC 3626, IETF Network Working Group, October 2003.
- [6] D. Johnson, D. Maltz, and J. Broch, “The Dynamic Source Routing Protocol (DSR) for mobile ad hoc networks for IPv4,” *No. RFC 4728*, 2007.
- [7] V. Park and M. Corson, “A Highly Adaptive Distributed Routing Algorithm for Mobile Wireless Networks,” in *Proc. of IEEE INFOCOM*, vol. 3, pp. 1405–1413, 1997.
- [8] C. Perkins and P. Bhagwat, “Highly Dynamic Destination-Sequenced Distance-Vector Routing (DSDV) for Mobile Computers,” *ACM SIGCOMM Computer Communications Review*, vol. 24, no. 4, pp. 234-244, 1994.
- [9] H. Narra, et al. “Destination-Sequenced Distance Vector (DSDV) Routing Protocol Implementation in NS-3,” in *Proc. of the 4th International ICST Conference on Simulation Tools and Techniques. ICST*, 2011.
- [10] D. Shin, H. Yoo, and D. Kim, “EMDOR: Emergency Message Dissemination with ACK-overhearing based Retransmission,” in *Proc. IEEE Int’l Conf. Ubiquitous and Future Networks (ICFUN’09)*, 2009, pp. 230–234.

- [11] N. Patal, D. Culler, and S. Shenker, “Trickle: A Self Regulating Algorithm for Code Propagation and Maintenance in Wireless Sensor Networks,” Comput. Science Division, University of California, 2003, pp. 15–28.
- [12] R. Poor, “Gradient Routing in Ad hoc Networks,” 2000.
- [13] R. Poor, Z. Smith, M. Paris, A. Wheeler, and R. Kelsey, “Ad hoc Wireless Network using Gradient Routing,” *U.S. Patent Application 10/457,205*.
- [14] I. F. Akyildiz and X. Wang, “A Survey on Wireless Mesh Networks,” *IEEE Commun. Mag.*, vol. 43, no. 9, pp. s23 – s30, Sept. 2005.
- [15] Q. Fang, J. Gao, L. J. Guibas, V. De Silva, and L. Zhang, “GLIDER: Gradient Landmark-based Distributed Routing for Sensor Networks,” in *Proc. IEEE INFOCOM 2005*, 2005, pp. 339–350.
- [16] B. Karp and H. T. Kung, “GPSR: Greedy Perimeter Stateless Routing for Wireless Networks,” in *ACM Int’l Conf. Mobile Computing and Networking (MobiCom’00)*, pp. 243–254, 2000.
- [17] N. Baccour, A. Koubâa, L. Mottola, M. A. Zúniga, H. Youssef, C. A. Boano, and M. Alves, “Radio Link Quality Estimation in Wireless Sensor Networks: A Survey,” *ACM Trans. Sensor Netw. (TOSN)*, vol. 8, no. 4:34, Sept. 2012.

- [18] D. Aguayo, J. Bicket, S. Biswas, G. Judd, and R. Morris, "Link-level Measurements from an 802.11b Mesh Network," *ACM SIGCOMM Comput. Commun. Review*, vol. 34, no. 4, pp. 121–132, Oct. 2004.
- [19] Nakagami, M., "The m-distribution - A General Formula of Intensity Distribution of Rapid Fading," *Statistical Method of Radio Propagation*, pp. 3–36, Pergamon Press: Oxford, U.K., 1960.
- [20] X. Zhang and G. Kang, "Chorus: Collision Resolution for Efficient Wireless Broadcast," in *IEEE INFOCOM 2010*, pp. 1–9, 2010.
- [21] N. Sadagopan, F. Bai, B. Krishnamachari, and A. Helmy, "PATHS: Analysis of Path Duration Statistics and Their Impact on Reactive MANET Routing Protocols," in *Proc. ACM Int'l Conf. Mobile Ad Hoc Networking and Computing (MobiHoc'03)*, 2003, pp. 245–256.
- [22] B. Sklar, "Rayleigh Fading Channels in Mobile Digital Communication Systems. I. Characterization," *IEEE Commun. Mag.*, vol. 35, no. 7, pp. 90–100, Jul. 1997.
- [23] C. Bettstetter, G. Resta, and P. Santi, "The Node Distribution of the Random Waypoint Mobility Model for Wireless Ad hoc Networks," *IEEE Trans. Mobile computing*, vol. 2, no. 3, pp. 257–269, Jul.-Sept. 2003.

- [24] M. T. Goodrich and R. Tamassia, “Algorithm Design,” 2002.
- [25] R. V. Glabbeek, P. Höfner, W. L. Tan, and M. Portmann, “Sequence Numbers Do Not Guarantee Loop Freedom - AODV Can Yield Routing Loops -,” in *Proc. ACM Int’l Symp. Modeling, analysis, and simulation of wireless and mobile systems (MSWiM’13)*, 2013, pp. 91–100.
- [26] W.R. Heinzelman, J. Kulik, and H. Balakrishnan, “Adaptive Protocols for Information Dissemination in Wireless Sensor Networks,” in *Proc. ACM/IEEE Int’l Conf. Mobile Computing and Networking (MobiCom’99)*, 1999, pp. 174–185.
- [27] H. Nishiyama, M. Ito, and N. Kato, “Relay-by-Smartphone: Realizing Multihop Device-to-Device Communications,” *IEEE Commun. Mag.*, vol. 52, no. 4, pp. 56–65, Apr. 2014.
- [28] A. Izaddoost and S. S. Heydari, “Enhancing Network Service Survivability in Large-Scale Failure Scenarios,” *J. of Commun. and Netw.*, vol. 16, no. 5, Oct. 2014.
- [29] A. S. Tanenbaum, “Computer Networks,” Prentice Hall, 1996, 3rd Ed.
- [30] K. Tang and M. Gerla, “MAC Reliable Broadcast in Ad hoc Networks,” in *Proc. IEEE Military Commun. Conf. (MILCOM’01)*, Oct. 2001, pp. 1008–1013.

- [31] M. T. Sun, L. Huang, A. Arora, and T. H. Lai, “Reliable MAC layer Multicast in IEEE 802.11 Wireless Networks,” *Wireless Commun. and Mobile Computing*, vol. 3, no. 4, pp. 439–453, Jun. 2003.
- [32] S. T. Sheu, Y. Tsai, and J. Chen, “A Highly Reliable Broadcast Scheme for IEEE 802.11 Multi-hop Ad hoc Networks,” in *Proc. IEEE Int’l Conf. on Commun. (ICC’02)*, May 2002, pp. 610–615.
- [33] C. Y. Chiu, E. K. Wu, and G. H. Chen, “A Reliable and Efficient MAC layer Broadcast Protocol for Mobile Ad hoc Networks,” *IEEE Trans. Vehicular Technology*, vol. 56, no. 4, pp. 2296–2305, Jul. 2007.
- [34] A. Dutta, D. Saha, D. Grunwald, and D. Sicker, “SMACK- A SMart ACKnowledgment Scheme for Broadcast Messages in Wireless Networks,” *ACM SIGCOMM Comput. Communication Review*, vol. 39, no. 4, pp. 15–26, 2009.
- [35] A. Sobeih, H. Baraka, and A. Fahmy, “ReMHoc: A Reliable Multicast Protocol for Wireless Mobile Multihop Ad hoc Networks,” in *Proc. Consumer Commun. and Networking Conf. (CCNC’04)*, 2004, pp. 146–151.
- [36] E. Pagani and G. P. Rossi, “Reliable Broadcast in Mobile Multihop Packet Networks,” in *Proc. ACM/IEEE Int’l Conf. Mobile*

- Computing and Networking (MobiCom'97)*, 1997, pp. 34–42.
- [37] H. Lim and C. Kim, “Flooding in Wireless Ad hoc Networks,” *Comput. Commun.*, vol. 24, no. 3, pp.353–363, 2001.
- [38] B. Blywis, M. Gnes, F. Juraschek, S. Hofmann, “Gossip routing in wireless mesh networks,” in *Proc. Int’l Symp. Personal Indoor and Mobile Radio Commun. (PIMRC’10)*, 2010, pp.1572–1577.
- [39] W. Lou and J. Wu, “Toward Broadcast Reliability in Mobile Ad Hoc Networks with Double Coverage,” *IEEE Trans. Mobile Computing*, vol. 6, no. 2, pp.148–163, Feb. 2007.
- [40] X. Y. Li, K. Moaveninejad, and O. Frieder, “Regional Gossip Routing for Wireless Ad hoc Networks,” *Mobile Networks and Applications*, vol. 10, no. 1-2, pp. 61–77, Feb. 2005.
- [41] Y. C. Tseng, S. Y. Ni, Y. S. Chen, and J. P. Sheu, “The Broadcast Storm Problem in a Mobile Ad hoc Network,” *Wireless Networks*, vol. 8, no. 2-3, pp. 153–167, Mar. 2002.
- [42] J. Fang et al., “Fine-grained channel access in wireless LAN,” *IEEE/ACM Trans. Netw.*, vol. 21, no. 3, pp. 772–787, Jun. 2013.
- [43] S. Sen, R. R. Choudhury, and S. Nelakuditi, “No Time to Countdown: Migrating Backoff to the Frequency Domain,” in *Proc. ACM/IEEE Int’l Conf. Mobile Computing and Networking (MobiCom’11)*, 2011, pp. 241–252.

- [44] Z. J. Haas, J. Y. Halpern, and L. Li, “Gossip-Based Ad Hoc Routing,” *IEEE/ACM Trans. Netw.*, vol. 14, no. 3, pp. 479–491, June 2006.
- [45] D. G. Reina, S. L. Toral, P. Johnson, and F. Barrero, “A Survey on Probabilistic Broadcast Schemes for Wireless Ad hoc Networks,” *Ad Hoc Networks*, vol. 25, pp. 263–292, Feb. 2015.
- [46] M. Abolhasan, T. Wysocki, and E. Dutkiewicz, “A Review of Routing Protocols for Mobile Ad hoc Networks,” *Elsevier Ad hoc Networks*, vol. 2, no. 1., pp. 1–22, Jan. 2004.
- [47] M. Takai, J. Martin, and R. Bagrodia, “Effects of Wireless Physical Layer Modeling in Mobile Ad hoc Networks,” in *Proc. ACM Int’l Symp. Mobile Ad Hoc Networking and Computing (MobiHoc’01)*, 2001, pp. 87–94.
- [48] K. W. Chin, “The Behavior of MANET Routing Protocols in Realistic Environments,” in *Proc. IEEE Asia-Pacific Conf. Commun.*, 2005, pp. 906–910.
- [49] F. Ye, G. Zhong, S. Lu, and L. Zhang, “Gradient Broadcast: A Robust Data Delivery Protocol for Larger Scale Sensor Networks,” *Wireless Networks*, vol. 11., no. 3, pp. 285 – 298, 2005.
- [50] M. Heissenbüttel, T. Braun, T. Bernoulli, and M. Wälchli, “BLR: Beacon-less Routing Algorithm for Mobile Ad hoc Net-

- works,” *Comp. Commun.*, vol. 27, no. 11, pp. 1076–1086, Jul. 2004.
- [51] P. Huang, H. Chen, G. Xing, and Y. Tan, “SGF: A State-free Gradient based Forwarding Protocol for Wireless Sensor Networks,” *ACM Trans. Sensor Networks (TOSN)*, vol. 5, no. 2: 14, 2009.
- [52] D. S. De Couto, D. Aguayo, J. Bicket, and R. Morris, “A High-throughput Path Metric for Multi-hop Wireless Routing,” *Wireless Networks*, vol. 11, no. 4, pp. 419–434, Jul. 2005.
- [53] C. E. Koksal and H. Balakrishnan, “Quality-aware Routing Metrics for Time-varying Wireless Mesh Networks,” in *IEEE J. Selected Area in Commun.*, vol. 24, no. 11, Nov. 2006.
- [54] R. Draves, J. Padhye, and B. Zill, “Comparison of Routing Metrics for Stasis Multi-hop Wireless Networks,” *ACM SIGCOMM Comp. Commun. Review*, vol. 34, no. 4, pp. 133–144, Oct. 2004.
- [55] D. Kotz, C. Newport, R. Gray, J. Liu, Y. Yuan, and C. Elliott, “Experimental Evaluation of Wireless Simulation Assumptions,” in *Proc. ACM Int’l Symp. Modeling, analysis, and simulation of wireless and mobile systems (MSWiM’13)*, 2013, pp. 91–100.
- [56] G. Pei and T. R. Henderson, “Validation of OFDM Error Rate Mode in ns-3,” *Boeing Research Technology*, 2010, pp. 1–15.

- [57] R. Maheshwari, J. Cao, and S. R. Das, “Physical Interference Modeling for Transmission Scheduling on Commodity WiFi Hardware,” in *Proc. IEEE Conf. Comput. Commun. (INFOCOM’09)*, 2009, pp. 2661–2665.
- [58] S. W. Kim, B.-S. Kim, and I. Lee, “MAC Protocol for Reliable Multicast over Multi-hop Wireless Ad Hoc Networks,” *J. of Commun. and Netw.*, vol. 14, no. 1, pp. 63–74, Feb. 2012.
- [59] Y.-J. Choi, S. Park, and S. Bahk, “Multichannel Random Access in OFDMA Wireless Networks,” *IEEE J. Sel. Areas Commun.*, vol. 24, no. 3, pp. 603–613, Mar. 2006.
- [60] IEEE Standard for Local Area and Metropolitan Area Networks Part 11. IEEE Std 802.11-2007
- [61] L. Litwin and M. Pugal, “The Principle of OFDM,” *RF signal processing*, vol.2, pp. 30–48, Jan. 2001.
- [62] B. Williams and T. Camp, “Comparison of Broadcasting Techniques for Mobile Ad Hoc Networks,” in *ACM Int’l Symp. Mobile Ad Hoc Networking and Computing (MobiHoc’02)*, 2002, pp. 194–205.
- [63] Ettus Research LLC, “Universal Software Radio Peripheral (USRP),” <http://www.ettus.com/>.
- [64] The ns-3 Network Simulator. <http://www.nsnam.org>, 2014.

국문초록

무선 이동 애드 혹 네트워크(MANET)는 특정 지역 내에 무작위로 분포된 무선 통신이 가능한 단말들로 구성된 네트워크이다. MANET의 가장 큰 특징은 각 단말들이 별도의 네트워크 기반 시설 없이 동적으로 네트워크를 구성하여 통신 서비스를 제공해야 한다는 점이다. 이때, 각 단말들의 신호 송신 범위에는 제한이 있기 때문에 데이터 트래픽 서비스에 있어서 소스 노드와 목적지 노드 사이의 중간 노드들이 해당 트래픽을 포워딩하는 라우팅 동작이 필요한 경우가 많다. 본 논문에서는 단말 간 멀티 홉 통신이 요구되는 MANET 환경에서 브로드캐스트 및 유니캐스트 데이터 트래픽을 안정적으로 서비스하기 위한 라우팅 방법을 제안한다.

첫 번째 부분에서는 직교 주파수 분할 다중 방식 (OFDM) 기반 무선 송수신기를 사용하는 단말들로 구성된 MANET에서 서브캐리어 수준의 톤 신호를 활용한 브로드캐스트 프로토콜을 제안한다. 제안 방식에서는 소스 노드에서 발생한 브로드캐스트 패킷의 일렬 번호를 특정 서브캐리어의 톤 신호들과 연관시켜, 수신단 기반의 패킷 재전송 및 취소 동작을 매우 낮은 수준의 제어 부하로 구현한다. 이를 통하여 보다 브로드캐스트 서비스의 안정성과 효율성을 동시에 높일 수 있다.

두 번째 부분에서는 MANET에서의 유니캐스트 서비스를 위한 대표적인 두 방식 (홉-바이-홉 라우팅, 경사도 라우팅)을 소개하고, 노드 이동성 및 신호 감쇠가 존재하는 상황에서도 안정적인 유니캐스트 서비스를 제공할 수 있도록 기존 경사도 라우팅 프로토콜을 재설계한다. 제안 방식의 핵심 요소는 주기적인 제어 신호 플래딩 및 신호 대 잡음비를 활용하여 각 노드에서 경사도 라우팅에 필요한 비용을 계산하는 것이다. 동작 분석 및 모의 실험 결과, 제안 방식이 기존에 존재하는 홉-바이-홉 라우팅 프로토콜들에 비해 보다 안정적인 유니캐스트 성능을 보여줌을 확인하였다.

세 번째 부분에서는 하나의 게이트웨이 노드와 다수의 일반 단말들로 이루어진 계층적 형태의 MANET에서 효과적인 상향링크 (단말에서 게이트웨이로 향하는 트래픽) 및 하향링크 (게이트웨이에서 단말로 향하는 트래픽) 유니캐스트 서비스를 위한 방법을 제시한다. 상향링크를 위해서는 톤 신호 기반의 비용 설정을 활용한 경사도 라우팅 방식을 제안하고, 하향링크에서는 상향링크 전송이력과 상향링크를 위한 비용을 함께 활용한 경사도 라우팅 방식을 제안한다. 이를 통하여 비용 관리 오버헤드를 최소화하면서 상향링크 및 하향링크 유니캐스트 서비스를 제공 할 수 있다.

주요어 : 무선 이동 애드 혹 네트워크, 경사도 라우팅, 브로드캐스트, 유니캐스트

학 번 : 2010-20743